arXiv:1510.08336v2 [math.NA] 1 Aug 2016

Tight error bounds for rank-1 lattice sampling in spaces of hybrid mixed smoothness

Glenn Byrenheid [†] Lutz Kämmerer[*] Tino Ullrich[†]
Toni Volkmer[*]

We consider the approximate recovery of multivariate periodic functions from a discrete set of function values taken on a rank-s integration lattice. The main result is the fact that any (non-)linear reconstruction algorithm taking function values on a rank-s lattice of size M has a dimension-independent lower bound of $2^{-(\alpha+1)/2}M^{-\alpha/2}$ when considering the optimal worst-case error with respect to function spaces of (hybrid) mixed smoothness $\alpha > 0$ on the d-torus. We complement this lower bound with upper bounds that coincide up to logarithmic terms. These upper bounds are obtained by a detailed analysis of a rank-1 lattice sampling strategy, where the rank-1 lattices are constructed by a component–by–component (CBC) method. This improves on earlier results obtained in [25] and [27]. The lattice (group) structure allows for an efficient approximation of the underlying function from its sampled values using a single one-dimensional fast Fourier transform. This is one reason why these algorithms keep attracting significant interest. We compare our results to recent (almost) optimal methods based upon samples on sparse grids.

Keywords and phrases : approximation of multivariate functions, trigonometric polynomials, hyperbolic cross, lattice rule, fast Fourier transform, dominating mixed smoothness, rank-1 lattices

AMS Mathematics Subject Classification 2000: 65T40, 42A10, 65D30, 65D32, 68Q17, 68Q25, 42B35, 65T50, 65Y20.

[*]Technische Universität Chemnitz, Faculty of Mathematics, 09107 Chemnitz, Germany
{lutz.kaemmerer, toni.volkmer}@mathematik.tu-chemnitz.de
[†]Hausdorff Center for Mathematics, Endenicher Allee 62, 53115 Bonn, Germany
{glenn.byrenheid, tino.ullrich}@hcm.uni-bonn.de

1 Introduction

This paper deals with the reconstruction of multivariate periodic functions from a discrete set of M function values along rank-1 lattices. Such lattices are widely used for the efficient numerical integration of multivariate periodic functions since the 1950ies [1, 21, 29, 35, 6] and represent a well-distributed set of points in $[0,1)^d$. A rank-1 lattice with $M \in \mathbb{N}$ points and generating vector $\boldsymbol{z} \in \mathbb{Z}^d$ is given by

$$\Lambda(\boldsymbol{z}, M) := \left\{ \frac{j}{M}\boldsymbol{z} \bmod \mathbf{1} \colon j = 0, \ldots, M-1 \right\}.$$

In this paper we will show that restricting the set of available discrete information to samples from a rank-s lattice, cf. [35], seriously affects the rate of convergence of a corresponding worst-case error with respect to classes of functions with (hybrid) mixed smoothness $\alpha > 0$. To be more precise, for any (possibly nonlinear) reconstruction procedure from sampled values along rank-s lattices we can find a function in the periodic Sobolev spaces $\mathcal{H}^{\alpha}_{\mathrm{mix}}$ such that the $L_2(\mathbb{T}^d)$ mean square error is at least $2^{-(\alpha+1)/2} M^{-\alpha/2}$. In contrast to that, it has been proved recently, that the sampling recovery from (energy) sparse grids leads to much better convergence rates, namely $M^{-\alpha}$ in the main term, see [33, 41, 4].

Subsequently, we study particular reconstructing algorithms, which are based on the naive approach of approximating the potentially "largest" Fourier coefficients (integrals) with the same rank-1 lattice rule. Despite the lacking asymptotical optimality, recovery from so-called reconstructing rank-1 lattices, cf. [15, 18], has some striking advantages.

First, the matrix of the underlying linear system of equations has orthogonal columns due to the group structure [2] and the reconstructing property of the used rank-1 lattices. Consequently, the computation is stable, cf. [17, 15].

Second, the CBC strategy [14, Tab. 3.1] provides a search method for a reconstructing rank-1 lattice which allows for the computation of the approximate Fourier coefficients belonging to frequencies lying on potentially unstructured sets. Besides a basic structure, e.g. generalized hyperbolic crosses, additional sparsity in the structure of the set of basis functions can be easily incorporated and may considerably reduce the number of required samples, e.g. see [18, Example 6.1].

Last, the approximate reconstruction can be efficiently performed using the sampled values of the underlying function and applying a single one-dimensional fast Fourier transform, cf. Algorithm 8.1 and [28, 2]. This idea has already been investigated by many authors including two of the present ones, see [37, 25, 26, 27, 18]. The arithmetic complexity is $\mathcal{O}(M \log M)$, and thus almost linear in the number of used sampling values.

The above mentioned advantages motivate a refined error analysis for the upper bounds which results in the observation that for the rank-1 lattice sampling the lower bound $M^{-\alpha/2}$ is sharp in the main order. It is important to mention that the rate $M^{-\alpha/2}$ is present in any dimension $d \geq 2$. Hence, the proposed naive but fast reconstruction algorithm is already more accurate than a comparable full tensor grid in case $d > 2$ yielding the order $M^{-\alpha/d}$. Moreover, the comparison to the mentioned sparse grid techniques is not completely hopeless since neither the asymptotical behavior of the approximation error tells anything about small values of M (so-called preasymptotics), which is indeed relevant for practical issues, nor is the computational cost for computing the sparse grid approximant completely reflected in the (optimal) main rate $M^{-\alpha}$, cf. [23, 24, 22]. This is the reason why these algorithms keep attracting more and more interest recently.

We consider the rate of convergence in the number of lattice points M of the worst-case error with respect to periodic Sobolev spaces with bounded mixed derivatives in L_2. These classes are given by

$$\mathcal{H}^{\alpha}_{\mathrm{mix}}(\mathbb{T}^d) = \Big\{ f \in L_2(\mathbb{T}^d) : \|f|\mathcal{H}^{\alpha}_{\mathrm{mix}}(\mathbb{T}^d)\|^2 := \sum_{\|\boldsymbol{m}\|_\infty \le \alpha} \|D^{\boldsymbol{m}} f\|_2^2 < \infty \Big\}, \tag{1.1}$$

where $\alpha \in \mathbb{N}$ denotes the mixed smoothness of the space. In order to quantitatively assess the quality of the proposed approximation, we introduce specifically tailored minimal worst-case errors $g_M^{\mathrm{latt}_1}(\mathcal{F}, Y)$ with respect to the function class $\mathcal{F}$ and the error in the norm of the function class Y. Our main result in case $\mathcal{F} = \mathcal{H}^{\alpha}_{\mathrm{mix}}(\mathbb{T}^d)$ and $Y = L_2(\mathbb{T}^d)$ reads as follows

$$M^{-\alpha/2} \lesssim g_M^{\mathrm{latt}_1}(\mathcal{H}^{\alpha}_{\mathrm{mix}}(\mathbb{T}^d), L_2(\mathbb{T}^d)) \lesssim M^{-\alpha/2} (\log M)^{\frac{d-2}{2}\alpha + \frac{d-1}{2}}, \quad M \in \mathbb{N}.$$

To be more precise, we use the following definition for sampling numbers along rank-1 lattice nodes

$$g_M^{\mathrm{latt}_1}(\mathcal{F}, Y) := \inf_{\boldsymbol{z} \in \mathbb{Z}^d} \mathrm{Samp}_{\Lambda(\boldsymbol{z}, M)}(\mathcal{F}, Y), \quad M \in \mathbb{N},$$

where we put for $\mathcal{G} := \{\boldsymbol{x}^1, ..., \boldsymbol{x}^M\} \subset \mathbb{T}^d$

$$\mathrm{Samp}_{\mathcal{G}}(\mathcal{F}, Y) := \inf_{A : \mathbb{C}^M \to Y} \sup_{\|f|\mathcal{F}\| \le 1} \Big\| f - A\big(f(\boldsymbol{x}^i)\big)_{i=1}^M \Big\|_Y .$$

Here we allow as well non-linear reconstruction operators $A \colon \mathbb{C}^M \to Y$. The general (non-linear) sampling numbers are defined as

$$g_M(\mathcal{F}, Y) := \inf_{\mathcal{G}} \mathrm{Samp}_{\mathcal{G}}(\mathcal{F}, Y), \quad M \in \mathbb{N},$$

for arbitrary sets of sampling nodes $\mathcal{G} := \{\boldsymbol{x}^1, ..., \boldsymbol{x}^M\} \subset \mathbb{T}^d$ and are sometimes also referred to as "optimal sampling recovery". These quantities are not the central focus of this paper, they rather serve as benchmark quantity. If the reconstruction operator A is supposed to be linear then we will use the notation $g_M^{\mathrm{lin}}(\mathcal{F}, Y)$. These quantities are well studied up to some prominent logarithmic gaps (cf. 3rd column in Table 1.2, 1.3 and 1.4). For an overview we refer to [4] and the references therein. Additionally, let us mention the work of Temlyakov [40, 39], Griebel et al. [3, 10, 11], Dinh [7, 9, 4] , Sickel [31, 32, 33, 34, 4], Ullrich [33, 41, 34, 4].

The main goal of this paper is to study the quantities $g_M^{\mathrm{latt}_1}(\mathcal{F}, Y)$ in several different approximation settings. At first, we measure the error in $Y = L_q(\mathbb{T}^d)$ with $2 \le q \le \infty$. In addition, we consider worst-case errors measured in isotropic Sobolev spaces $Y = \mathcal{H}^{\gamma}(\mathbb{T}^d)$ (defined as $\mathcal{H}^{\gamma}(\mathbb{T}^d) := \mathcal{H}^{0,\gamma}(\mathbb{T}^d)$ in (1.2) below) which includes the energy-norm $\mathcal{H}^1(\mathbb{T}^d)$ relevant for Galerkin approximation schemes. Multivariate functions are taken from fractional ($\alpha > 0$) Sobolev spaces $\mathcal{F} = \mathcal{H}^{\alpha}_{\mathrm{mix}}(\mathbb{T}^d)$ of mixed smoothness and even more general hybrid type Sobolev spaces $\mathcal{F} = \mathcal{H}^{\alpha,\beta}(\mathbb{T}^d)$, introduced by Griebel and Knapek [11]. In fact, Yserentant [42] proved that eigenfunctions of the positive spectrum of the electronic Schrödinger operators have a mixed type regularity. Even more, their regularity can be described as a combination of mixed and isotropic (hybrid) smoothness

$$\mathcal{H}^{\alpha,\beta}(\mathbb{T}^d) = \Big\{ f \in L_2(\mathbb{T}^d) : \|f|\mathcal{H}^{\alpha,\beta}(\mathbb{T}^d)\|^2 := \sum_{\|\boldsymbol{m}\|_\infty \le \alpha} \sum_{\|\boldsymbol{n}\|_1 \le \beta} \|D^{\boldsymbol{m}+\boldsymbol{n}} f\|_2^2 < \infty \Big\}. \tag{1.2}$$

A related concept is given by anisotropic mixed Sobolev smoothness

$$\mathcal{H}^{\boldsymbol{\alpha}}_{\mathrm{mix}}(\mathbb{T}^d) = \Big\{ f \in L_2(\mathbb{T}^d) : \|f|\mathcal{H}^{\boldsymbol{\alpha}}_{\mathrm{mix}}(\mathbb{T}^d)\|^2 := \sum_{\substack{m_i \le \alpha_i \\ i=1,\dots,d}} \|D^{\boldsymbol{m}} f\|_2^2 < \infty \Big\}, \tag{1.3}$$

where the smoothness is characterized by vectors $\boldsymbol{\alpha} \in \mathbb{N}_0^d$. In fact, we have the representation

$$\mathcal{H}^{\alpha,\beta} = \bigcap_{i=1}^{d} \mathcal{H}^{\alpha\cdot\mathbf{1}+\beta\cdot\boldsymbol{e}_i}_{\mathrm{mix}},$$

where $\boldsymbol{e}_i$ is the i-th unit vector. The norms in (1.1), (1.2), (1.3) can be rephrased as weighted ℓ_2-sums of Fourier coefficients which is also the natural way to extend the spaces $\mathcal{H}^{\alpha,\beta}(\mathbb{T}^d)$ to fractional parameters, see (2.1) below. We extend methods from [17, 18] to obtain sharp bounds (up to logarithmic factors) for $g_M^{\mathrm{latt}_1}(\mathcal{H}^{\alpha,\beta}(\mathbb{T}^d), H^\gamma(\mathbb{T}^d))$, which show in particular that even non-linear reconstruction maps can not get below $c_{\alpha,\beta,\gamma,d} M^{-(\alpha+\beta-\gamma)/2}$. The upper bounds are obtained with a specific simple algorithm that approximates the "largest" Fourier coefficients (2.2) of the function with one fixed lattice rule, where the corresponding frequencies of the Fourier coefficients are determined by the function class. To this end, a so-called reconstructing rank-1 lattice [14, Ch. 3] is used, which is constructed via the component–by–component (CBC) strategy [36]. Similar strategies have already proved useful for numerical integration, see [36, 5, 6]. The basic idea behind is the construction of a generating vector $\boldsymbol{z}$ component-wise by iteratively increasing the dimension of the index set for which a reproduction property should hold.

Let us finally comment on some relevant earlier results in this direction. One of the first upper bounds for $g_M^{\mathrm{latt}_1}(\mathcal{H}^{\alpha}_{\mathrm{mix}}(\mathbb{T}^d), L_2(\mathbb{T}^d))$ has been obtained by Temlyakov in [37] for the Korobov lattice, which represents a rank-1 lattice with a generating vector $\boldsymbol{a} = (1, a, a^2, \dots, a^{d-1})$ for some integer a. He obtained the estimate

$$\mathrm{Samp}_{\Lambda(\boldsymbol{a},M)}(\mathcal{H}^{\alpha}_{\mathrm{mix}}(\mathbb{T}^d), L_2(\mathbb{T}^d)) \lesssim M^{-\alpha/2} (\log M)^{(d-1)(\alpha/2+1/2)}.$$

Further results that imply upper bounds for $g_M^{\mathrm{latt}_1}(\mathcal{H}^{\alpha}_{\mathrm{mix}}(\mathbb{T}^d), L_2(\mathbb{T}^d))$ have been proved in [25]. Rephrasing the error bounds in [25] depending on the number of lattice points M, we observe a rate of $M^{-(\alpha-\lambda)/2}$ for any $\lambda > 0$. In [27] the rank-1 lattice sampling error measured in $L_\infty(\mathbb{T}^d)$ is considered and the main rate $M^{-(\alpha-1/2-\lambda)/2}$ is obtained for every $\lambda > 0$. In [19] the technique used by Temlyakov [37] is expanded to model spaces $\mathcal{H}^{\alpha,\beta}(\mathbb{T}^d)$ with $\beta < 0$ and $\alpha + \beta > 1/2$, where the authors obtain the upper bound

$$g_M^{\mathrm{latt}_1}(\mathcal{H}^{\alpha,\beta}(\mathbb{T}^d), L_2(\mathbb{T}^d)) \lesssim M^{-(\alpha+\beta)/2}$$

without any further logarithmic dependence.

Contribution and main results. The first main contribution of the present paper is the lower bound

$$c_{\alpha,\beta,\gamma}\, M^{-(\alpha+\beta-\gamma)/2} \le g_M^{\mathrm{latt}_1}(\mathcal{H}^{\alpha,\beta}(\mathbb{T}^d), Y), \qquad c_{\alpha,\beta,\gamma} := 2^{-(\alpha+\beta-\gamma+1)/2},$$

for $Y \in \{L_2(\mathbb{T}^d) = \mathcal{H}^0(\mathbb{T}^d), \mathcal{H}^\gamma(\mathbb{T}^d), \mathcal{H}^\gamma_{\mathrm{mix}}(\mathbb{T}^d)\}$ and $\min\{\alpha, \alpha+\beta\} > \gamma \ge 0$, cf. Section 3. In the cases $Y \in \{L_2(\mathbb{T}^d), \mathcal{H}^\gamma(\mathbb{T}^d), \mathcal{H}^\gamma_{\mathrm{mix}}(\mathbb{T}^d)\}$ and $\alpha + \beta > \max\{\gamma, 1/2\}$ with $\beta \le 0$ and $\gamma \ge 0$,

Y	$g_M^{\mathrm{latt}_1}(\mathcal{H}^{\alpha,\beta}(\mathbb{T}^d), Y)$	$g_M(\mathcal{H}^{\alpha,\beta}(\mathbb{T}^d), Y)$
$L_2(\mathbb{T}^d), \mathcal{H}^\gamma(\mathbb{T}^d), \mathcal{H}^\gamma_{\mathrm{mix}}(\mathbb{T}^d)$	$\gtrsim M^{-\frac{\alpha+\beta-\gamma}{2}}$ (Proposition 3.3)	$\gtrsim M^{-(\alpha+\beta-\gamma)}$ [8] linear, [9] non-linear, non-periodic

Table 1.1: Lower bounds of sampling numbers for different sampling methods.

the upper bounds on the rank-1 lattice sampling rates match the general lower bounds up to logarithmic factors, cf. Sections 4, 5.

The second column in Table 1.1, 1.2 and 1.3 is headlined with $g_M^{\mathrm{latt}_1}(\mathcal{H}^{\alpha,\beta}(\mathbb{T}^d), Y)$ and presents lower and upper bounds on the sampling rates in various settings for sampling along reconstructing rank-1 lattices. Table 1.1 shows the lower bounds from Section 3. Table 1.2 deals with upper bounds in the model spaces $\mathcal{H}^\alpha_{\mathrm{mix}}(\mathbb{T}^d)$, whereas in Table 1.3 model spaces $\mathcal{H}^{\alpha,\beta}(\mathbb{T}^d)$ with negative isotropic smoothness parameter β are considered. The corresponding $L_2(\mathbb{T}^d)$ error estimate in the first table improves on the result obtained by Temlyakov in [37] by a logarithmic factor $(\log M)^{\alpha/2}$. In contrast to the rank-1 lattices constructed by the CBC strategy, the considerations by Temlyakov are based on rank-1 lattices of Korobov type. Smoothness parameters are chosen from $\beta < 0$, $\alpha + \beta > \max\{\gamma, 1/2\}$, $\gamma > 0$, and $2 < q < \infty$. Best known bounds are based on energy sparse grid sampling. References marked with * mean that the result is not stated there explicitly but follows with the same method therein. For our method the crucial property of the used rank-1 lattice sampling scheme is the reconstruction property (2.5). In order to construct such rank-1 lattices, one may use the CBC strategy [14, Tab. 3.1]. Additionally, in case $d = 2$ the Fibonacci lattice fulfills such a property. In both of these cases, we obtain the improved estimates as shown in Table 1.4. Smoothness parameters are chosen from $\alpha > 1/2$, $\alpha > \gamma > 0$. The upper bounds for $g_M^{\mathrm{latt}_1}$ are realized either by the Fibonacci or CBC-generated lattice. From the point of error estimates, the case $d = 2$ represents an interesting special case. We have sharp bounds and no logarithmic dependencies here, except in the case where we measure the error in a space with mixed regularity. Hence, lattice sampling turns out to be as good as sampling on the full tensor grid in $d = 2$. Last but not least, we consider the recovery of functions from $\mathcal{H}^{\boldsymbol{\alpha}}_{\mathrm{mix}}(\mathbb{T}^d)$ with anisotropic mixed smoothness. We consider smoothness vectors $\boldsymbol{\alpha} \in \mathbb{R}^d$ with first μ smallest smoothness directions, i.e.

$$\frac{1}{2} < \alpha_1 = \ldots = \alpha_\mu < \alpha_{\mu+1} \leq \ldots \leq \alpha_d.$$

Here we show for the L_∞ approximation error the bound

$$g_M^{\mathrm{latt}_1}(\mathcal{H}^{\boldsymbol{\alpha}}_{\mathrm{mix}}(\mathbb{T}^d), L_\infty(\mathbb{T}^d)) \lesssim M^{-(\alpha_1-\frac{1}{2})/2}(\log M)^{(\mu-1)(\alpha_1/2+1/4)}.$$

That means the exponent of the logarithm depends only on $\mu < d$ instead of d. Similar effects are also known for general linear approximation and sparse grid sampling, cf. [9, 38].

Notation. As usual, $\mathbb{N}$ denotes the natural numbers, $\mathbb{N}_0$ the non-negative integers, $\mathbb{Z}$ the integers and $\mathbb{R}$ the real numbers. With $\mathbb{T}$ we denote the torus represented by the interval $[0, 1)$. The letter d is always reserved for the dimension in $\mathbb{Z}$, $\mathbb{R}$, $\mathbb{N}$, and $\mathbb{T}$. For $0 < p \leq \infty$ and $\boldsymbol{x} \in \mathbb{R}^d$ we denote $\|\boldsymbol{x}\|_p = (\sum_{i=1}^d |x_i|^p)^{1/p}$ with the usual modification for $p = \infty$. The norm of an element $x \in X$ is denoted by $\|x|X\|$. If X and Y are two Banach spaces, the norm of an operator $A\colon X \to Y$ will be denoted by $\|A|X \to Y\|$. The symbol $X \hookrightarrow Y$ indicates

Y	$g_M^{\mathrm{latt}_1}(\mathcal{H}^\alpha_{\mathrm{mix}}(\mathbb{T}^d), Y)$	$g_M^{\mathrm{lin}}(\mathcal{H}^\alpha_{\mathrm{mix}}(\mathbb{T}^d), Y)$
$L_2(\mathbb{T}^d)$	$\lesssim M^{-\frac{\alpha}{2}} (\log M)^{\frac{d-2}{2}\alpha+\frac{d-1}{2}}$ (Theorem 4.4)	$\lesssim M^{-\alpha} (\log M)^{(d-1)(\alpha+\frac{1}{2})}$ [4, Theorem 6.10], sparse grid
$L_q(\mathbb{T}^d)$	$\lesssim M^{-\frac{\alpha-(\frac{1}{2}-\frac{1}{q})}{2}}$ $(\log M)^{\frac{d-2}{2}(\alpha-(\frac{1}{2}-\frac{1}{q}))+\frac{d-1}{2}}$ (Proposition 4.7)	$\asymp M^{-(\alpha-(\frac{1}{2}-\frac{1}{q}))}$ $(\log M)^{(d-1)(\alpha-(\frac{1}{2}-\frac{1}{q}))}$ [4, Theorem 6.10], sparse grid
$L_\infty(\mathbb{T}^d)$	$\lesssim M^{-\frac{\alpha-\frac{1}{2}}{2}} (\log M)^{\frac{d-2}{2}(\alpha-\frac{1}{2})+\frac{d-1}{2}}$ (Proposition 4.9)	$\asymp M^{-\alpha+\frac{1}{2}} (\log M)^{(d-1)\alpha}$ [4, Theorem 6.10], sparse grid
$\mathcal{H}^\gamma(\mathbb{T}^d)$	$\lesssim M^{-\frac{\alpha-\gamma}{2}} (\log M)^{\frac{d-2}{2}(\alpha-\gamma)+\frac{d-1}{2}}$ (Proposition 4.6)	$\asymp M^{-(\alpha-\gamma)}$ [4, Theorem 6.7], energy sparse grid
$\mathcal{H}^\gamma_{\mathrm{mix}}(\mathbb{T}^d)$	$\lesssim M^{-\frac{\alpha-\gamma}{2}} (\log M)^{\frac{d-2}{2}(\alpha-\gamma)+\frac{d-1}{2}}$ (Theorem 4.4)	$\asymp M^{-(\alpha-\gamma)} (\log M)^{(d-1)(\alpha-\gamma)}$ [4, Theorem 6.10], sparse grid

Table 1.2: Upper bounds of sampling numbers in the setting $\mathcal{H}^\alpha_{\mathrm{mix}}(\mathbb{T}^d) \to Y$ for different sampling methods. Smoothness parameters are chosen from $\alpha > \max\{\gamma, \frac{1}{2}\}$, $\gamma > 0$, and $2 < q < \infty$. The upper bounds on $g_M^{\mathrm{latt}_1}$ are realized by the CBC rank-1 lattice.

Y	$g_M^{\mathrm{latt}_1}(\mathcal{H}^{\alpha,\beta}(\mathbb{T}^d), Y)$	$g_M^{\mathrm{lin}}(\mathcal{H}^{\alpha,\beta}(\mathbb{T}^d), Y)$
$L_2(\mathbb{T}^d)$	$\lesssim M^{-\frac{\alpha+\beta}{2}}$ [19, Theorem 4.7]	$\asymp M^{-(\alpha+\beta)}$ [4, Theorem 6.10]
$L_q(\mathbb{T}^d)$	$\lesssim M^{-\frac{\alpha-(\frac{1}{2}-\frac{1}{q})+\beta}{2}} (\log M)^{\frac{d-2}{2}(\alpha-(\frac{1}{2}-\frac{1}{q})+\beta)}$ (Proposition 4.7)	$\lesssim M^{-(\alpha-(\frac{1}{2}-\frac{1}{q})+\beta)}$ [4, *]
$L_\infty(\mathbb{T}^d)$	$\lesssim M^{-\frac{\alpha+\beta-\frac{1}{2}}{2}}$ (Proposition 4.9)	$\lesssim M^{-(\alpha+\beta)+\frac{1}{2}}$ [4, *]
$\mathcal{H}^\gamma(\mathbb{T}^d)$	$\lesssim M^{-\frac{\alpha+\beta-\gamma}{2}} (\log M)^{\frac{d-2}{2}(\alpha+\beta-\gamma)}$ (Proposition 4.6)	$\asymp M^{-(\alpha+\beta-\gamma)}$ [4, Theorem 6.7]
$\mathcal{H}^\gamma_{\mathrm{mix}}(\mathbb{T}^d)$	$\lesssim M^{-\frac{\alpha+\beta-\gamma}{2}} (\log M)^{\frac{d-2}{2}(\alpha+\beta-\gamma)}$ (Theorem 4.4)	$\asymp M^{-(\alpha+\beta-\gamma)}$ [4, *]

Table 1.3: Upper bounds for sampling numbers for different sampling methods. Smoothness parameters are chosen from $\beta < 0$, $\alpha + \beta > \max\{\gamma, \frac{1}{2}\}$, $\gamma > 0$, and $2 < q < \infty$. Best known bounds based on energy sparse grid sampling. References marked with * means that the result is not stated there explicitly but follows with the same method therein.

that there is a continuous embedding from X into Y. The relation $a_n \lesssim b_n$ means that there is a constant $c > 0$ independent of the context relevant parameters such that $a_n \leq c\, b_n$ for all

Y	$g_M^{\mathrm{latt}_1}(\mathcal{H}^\alpha_{\mathrm{mix}}(\mathbb{T}^2), Y)$	$g_M^{\mathrm{lin}}(\mathcal{H}^\alpha_{\mathrm{mix}}(\mathbb{T}^2), Y)$
$L_2(\mathbb{T}^2)$	$\asymp M^{-\frac{\alpha}{2}}$ (Theorem 5.3)	$\lesssim M^{-\alpha}(\log M)^{\alpha+\frac{1}{2}}$ [4, Theorem 6.10], sparse grid
$L_\infty(\mathbb{T}^2)$	$\lesssim M^{-\frac{\alpha-\frac{1}{2}}{2}}$ (Proposition 5.6)	$\asymp M^{-\alpha+\frac{1}{2}}(\log M)^{\alpha}$ [4, Theorem 6.10], sparse grid
$\mathcal{H}^\gamma(\mathbb{T}^2)$	$\asymp M^{-\frac{\alpha-\gamma}{2}}$ (Theorem 5.3)	$\asymp M^{-(\alpha-\gamma)}$ [4, Theorem 6.7], energy sparse grid
$\mathcal{H}^\gamma_{\mathrm{mix}}(\mathbb{T}^2)$	$\lesssim M^{-\frac{\alpha-\gamma}{2}}(\log M)^{\frac{1}{2}}$ (Remark 5.4)	$\asymp M^{-(\alpha-\gamma)}(\log M)^{\alpha-\gamma}$ [4, Theorem 6.10], sparse grid

Table 1.4: Upper bounds for sampling rates for different sampling methods. Smoothness parameters are chosen from $\alpha > \frac{1}{2}$, $\alpha > \gamma > 0$. The upper bounds for $g_M^{\mathrm{latt}_1}$ are realized either by the Fibonacci or CBC-generated lattice.

n belonging to a certain subset of $\mathbb{N}$, often $\mathbb{N}$ itself. We write $a_n \asymp b_n$ if $a_n \lesssim b_n$ and $b_n \lesssim a_n$ holds.

2 Definitions and prerequisites

The well known fact that decay properties of Fourier coefficients of a periodic function f can be rephrased in smoothness properties of f motivates to define the weighted Hilbert spaces

$$\mathcal{H}^{\alpha,\beta}(\mathbb{T}^d) := \left\{ f \in L_2(\mathbb{T}^d) \colon \|f|\mathcal{H}^{\alpha,\beta}(\mathbb{T}^d)\|^2 := \sum_{\boldsymbol{k}\in\mathbb{Z}^d} |\hat{f}_{\boldsymbol{k}}|^2 (1+\|\boldsymbol{k}\|_2^2)^\beta \prod_{s=1}^d (1+|k_s|^2)^\alpha < \infty \right\}, \tag{2.1}$$

that mainly depend on the smoothness parameters $\alpha, \beta \in \mathbb{R}$, $\min\{\alpha, \alpha+\beta\} > 0$. It is easy to show that for integer $\alpha, \beta \in \mathbb{N}_0$ these spaces coincide with the spaces defined in (1.2). Furthermore in case $\alpha = 0$ and $\beta \geq 0$ these spaces coincide with isotropic Sobolev spaces, therefore we use the definition $\mathcal{H}^\beta(\mathbb{T}^d) := \mathcal{H}^{0,\beta}(\mathbb{T}^d)$. For $\alpha \geq 0$ and $\beta = 0$ the spaces $\mathcal{H}^{\alpha,0}(\mathbb{T}^d)$ coincide with $\mathcal{H}^\alpha_{\mathrm{mix}}(\mathbb{T}^d)$, i.e. with the Sobolev spaces of dominating mixed smoothness, and we use the definition $\mathcal{H}^\alpha_{\mathrm{mix}}(\mathbb{T}^d) := \mathcal{H}^{\alpha,0}(\mathbb{T}^d)$. Since we want to deal with sampling, we are interested in continuous functions.

Lemma 2.1. *Let $\alpha, \beta \in \mathbb{R}$ with $\min\{\alpha, \alpha+\beta\} > \frac{1}{2}$. Then*

$$\mathcal{H}^{\alpha,\beta}(\mathbb{T}^d) \hookrightarrow C(\mathbb{T}^d).$$

Proof. We refer to [4, Theorem 2.9]. ∎

The Fourier partial sum of a function $f \in L_1(\mathbb{T}^d)$ with respect to the frequency index set $I \subset \mathbb{Z}^d$, $|I| < \infty$, is defined by

$$S_I f := \sum_{\boldsymbol{k}\in I} \hat{f}_{\boldsymbol{k}} \mathrm{e}^{2\pi \mathrm{i} \boldsymbol{k}\cdot\circ},$$

where

$$\hat{f}_{\boldsymbol{k}} := \int_{\mathbb{T}^d} f(\boldsymbol{x}) \mathrm{e}^{-2\pi \mathrm{i} \boldsymbol{k}\cdot\boldsymbol{x}} \mathrm{d}\boldsymbol{x} \tag{2.2}$$

are the usual Fourier coefficients of f.

We approximate the Fourier coefficients $\hat{f}_{\boldsymbol{k}}$, $\boldsymbol{k} \in I$, based on sampling values taken at the nodes of a rank-1 lattice

$$\Lambda(\boldsymbol{z}, M) := \left\{ \frac{j}{M}\boldsymbol{z} \bmod \mathbf{1} \colon j = 0, \ldots, M-1 \right\} \subset \mathbb{T}^d,$$

where $\boldsymbol{z} \in \mathbb{Z}^d$ is the generating vector and $M \in \mathbb{N}$ is the lattice size. In particular, we apply the quasi-Monte Carlo rule defined by the rank-1 lattice $\Lambda(\boldsymbol{z}, M)$ on the integrand in (2.2), i.e.,

$$\hat{f}_{\boldsymbol{k}}^{\Lambda(\boldsymbol{z},M)} := \frac{1}{M} \sum_{j=0}^{M-1} f\Big(\frac{j}{M}\boldsymbol{z}\Big) \mathrm{e}^{-2\pi \mathrm{i} \frac{j}{M} \boldsymbol{k}\cdot\boldsymbol{z}}.$$

Accordingly, we define the rank-1 lattice sampling operator $S_I^{\Lambda(\boldsymbol{z},M)}$ by

$$S_I^{\Lambda(\boldsymbol{z},M)} f := \sum_{\boldsymbol{k}\in I} \hat{f}_{\boldsymbol{k}}^{\Lambda(\boldsymbol{z},M)} \mathrm{e}^{2\pi \mathrm{i} \boldsymbol{k}\cdot\circ}. \tag{2.3}$$

We call a rank-1 lattice $\Lambda(\boldsymbol{z}, M)$ *reconstructing rank-1 lattice* for the frequency index set $I \subset \mathbb{Z}^d$, $|I| < \infty$, if the sampling operator $S_I^{\Lambda(\boldsymbol{z},M)}$ reproduces all trigonometric polynomials with frequencies supported on I, i.e., $S_I^{\Lambda(\boldsymbol{z},M)} p = p$ holds for all trigonometric polynomials

$$p \in \Pi_I := \operatorname{span}\{\mathrm{e}^{2\pi \mathrm{i} \boldsymbol{k}\cdot\circ} \colon \boldsymbol{k} \in I\}. \tag{2.4}$$

The condition

$$\boldsymbol{k}^1 \cdot \boldsymbol{z} \not\equiv \boldsymbol{k}^2 \cdot \boldsymbol{z} \pmod{M} \quad \text{for all } \boldsymbol{k}^1, \boldsymbol{k}^2 \in I,\ \boldsymbol{k}^1 \neq \boldsymbol{k}^2, \tag{2.5}$$

has to be fulfilled in order to guarantee that $\Lambda(\boldsymbol{z}, M)$ is a reconstructing rank-1 lattice for the frequency index set I. One can show, that the condition in (2.5) is not only sufficient but also necessary. In the following sections, we frequently use the so-called difference set $\mathcal{D}(I)$ of a frequency index set $I \subset \mathbb{Z}^d$, $|I| < \infty$,

$$\mathcal{D}(I) := \left\{ \boldsymbol{k} \in \mathbb{Z}^d \colon \boldsymbol{k} = \boldsymbol{h}^1 - \boldsymbol{h}^2,\ \boldsymbol{h}^1, \boldsymbol{h}^2 \in I \right\}.$$

This definition allows for the reformulation of (2.5) in terms of the difference set $\mathcal{D}(I)$, i.e.,

$$\boldsymbol{k} \cdot \boldsymbol{z} \not\equiv 0 \pmod{M} \quad \text{for all } \boldsymbol{k} \in \mathcal{D}(I) \setminus \{\mathbf{0}\}. \tag{2.6}$$

Furthermore, we define the dual lattice

$$\Lambda(\boldsymbol{z}, M)^\perp := \{\boldsymbol{h} \in \mathbb{Z}^d \colon \boldsymbol{h} \cdot \boldsymbol{z} \equiv 0 \pmod{M}\}$$

of the rank-1 lattice $\Lambda(\boldsymbol{z}, M)$. We use this definition in order to characterize the reconstruction property of a rank-1 lattice $\Lambda(\boldsymbol{z}, M)$ for a frequency index set I. A rank-1 lattice $\Lambda(\boldsymbol{z}, M)$ is a reconstructing rank-1 lattice for the frequency index set I, $1 \leq |I| < \infty$, iff

$$\Lambda(\boldsymbol{z}, M)^\perp \cap \mathcal{D}(I) = \{\mathbf{0}\} \tag{2.7}$$

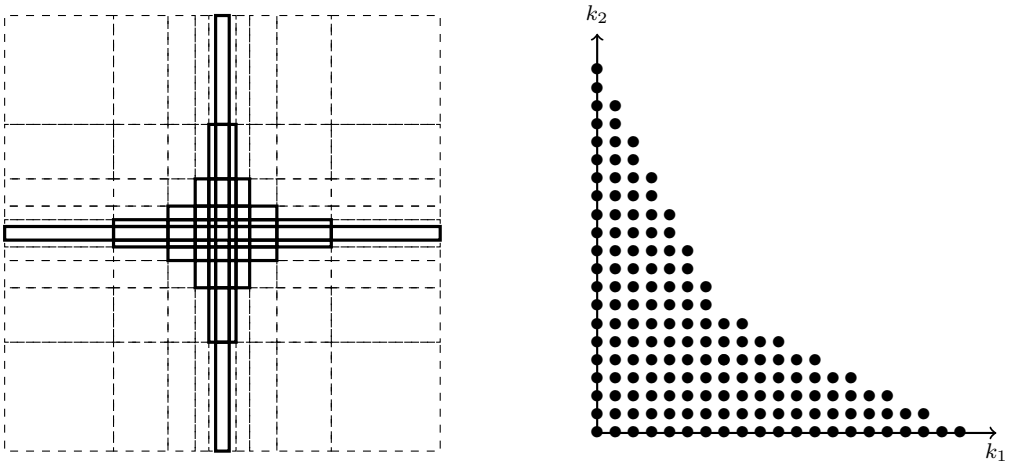

Figure 2.1: $H_4^{2,0}$ and $J_{20}^{2,0.5}$

holds. This means the conditions (2.5), (2.6) and (2.7) are equivalent, see also [15]. In order to approximate functions $f \in \mathcal{H}^{\alpha,\beta}(\mathbb{T}^d)$ using trigonometric polynomials, we have to carefully choose the spaces Π_I (cf. (2.4)) of these trigonometric polynomials. Clearly, the spaces Π_I are described by the corresponding frequency index set I. For technical reasons, we use so-called generalized dyadic hyperbolic crosses,

$$I = H_R^{d,T} := \bigcup_{\boldsymbol{j} \in J_R^{d,T}} Q_{\boldsymbol{j}}, \tag{2.8}$$

cf. Figure 2.1, where $R \geq 1$ denotes the refinement, $T \in [0,1)$ is an additional parameter,

$$J_R^{d,T} := \{\boldsymbol{j} \in \mathbb{N}_0^d \colon \|\boldsymbol{j}\|_1 - T\|\boldsymbol{j}\|_\infty \leq (1-T)R + d - 1\},$$

and $Q_{\boldsymbol{j}} := \times_{s=1}^d Q_{j_s}$ are sets of tensorized dyadic intervals

$$Q_j := \begin{cases} \{-1,0,1\} & : \ j = 0, \\ ([-2^j, -2^{j-1}-1] \cup [2^{j-1}+1, 2^j]) \cap \mathbb{Z} & : \ j > 0, \end{cases} \tag{2.9}$$

cf. [20].

Lemma 2.2. *Let the dimension $d \in \mathbb{N}$, the parameter $T \in [0,1)$, and the refinement $R \geq 1$, be given. Then, we estimate the cardinality of the index set $H_R^{d,T}$ by*

$$|H_R^{d,T}| \asymp \begin{cases} 2^R R^{d-1} & : \ T = 0, \\ 2^R & : \ 0 < T < 1. \end{cases}$$

Proof. The assertion for the upper bound follows directly from [11, Lemma 4.2]. For a proof including the lower bound we refer to [4, Lemma 6.6]. ∎

Having fixed the index set $I = H_R^{d,T}$ an important question is the existence of a reconstructing lattice for it. If there is such a lattice, out of how many points does it consist? Can we explicitly construct it? The following lemma answers these questions.

Lemma 2.3. *Let the parameters $T \in [0,1)$, $R \geq 1$, and the dimension $d \in \mathbb{N}$, $d \geq 2$, be given. Then, there exists a reconstructing rank-1 lattice $\Lambda(\boldsymbol{z}, M)$ for $H_R^{d,T}$ which fulfills*

$$2^{2R-2} \leq M \lesssim \begin{cases} 2^{2R} & : \ T > 0, \\ 2^{2R} R^{d-2} & : \ T = 0. \end{cases}$$

Moreover, each reconstructing rank-1 lattice $\Lambda(\boldsymbol{z}, M)$ for $H_R^{d,T}$ fulfills the lower bound.

Proof. For $T = 0$, a detailed proof of the bounds can be found in [13]. In the case $T \in (0,1)$, one proves the lower bound using the same way as used for $T = 0$. The corresponding upper bound follows directly from [15, Cor. 1] and $H_R^{d,T} \subset [-|H_R^{d,T}|, |H_R^{d,T}|]^d$ and $|H_R^{d,T}| \lesssim 2^R$. ■

A lattice fulfilling these properties can be explicitly constructed using a component-by-component (CBC) optimization strategy for the generating vector $\boldsymbol{z}$. For more details on that algorithm we refer to [14, Ch. 3].

3 Lower bounds and non-optimality

In this chapter we study lower bounds for the rank-1 lattice sampling numbers $g_M^{\mathrm{latt}_1}(\mathcal{H}^{\alpha,\beta}(\mathbb{T}^d), \mathcal{H}^{\gamma}(\mathbb{T}^d))$ and $g_M^{\mathrm{latt}_1}(\mathcal{H}^{\alpha,\beta}(\mathbb{T}^d), \mathcal{H}^{\gamma}_{\mathrm{mix}}(\mathbb{T}^d))$. At first we show, that each rank-1 lattice $\Lambda(\boldsymbol{z}, M)$, $\boldsymbol{z} \in \mathbb{Z}^d$, $d \geq 2$, and $M \in \mathbb{N}$, has at least one aliasing pair of frequency indices $\boldsymbol{k}^1, \boldsymbol{k}^2$ within the two-dimensional axis cross

$$\mathrm{X}_{\sqrt{M}}^d := \{\boldsymbol{h} \in \mathbb{Z}^2 \times \underbrace{\{0\} \times \ldots \times \{0\}}_{d-2 \text{ times}} \colon \|\boldsymbol{h}\|_1 = \|\boldsymbol{h}\|_\infty \leq \sqrt{M}\}.$$

For illustration, we depict X_8^3 in Figure 3.1a. We can even show a more general result.

Lemma 3.1. *Let $\mathcal{X} := \{\boldsymbol{x}_j \in \mathbb{T}^d \colon j = 0, \ldots, M-1\}$, $d \geq 2$, be a sampling set of cardinality $|\mathcal{X}| = M$. In addition, we assume that*

$$\sum_{j=0}^{M-1} \mathrm{e}^{2\pi \mathrm{i} \boldsymbol{k} \cdot \boldsymbol{x}_j} \in \{0, M\} \text{ for all } \boldsymbol{k} \in P_{\sqrt{M}}^d := \{-\left\lfloor \sqrt{M} \right\rfloor, \ldots, \left\lfloor \sqrt{M} \right\rfloor\}^2 \times \underbrace{\{0\} \times \ldots \times \{0\}}_{d-2 \text{ times}}.$$

Then there exist at least two distinct indices $\boldsymbol{k}^1, \boldsymbol{k}^2 \in \mathrm{X}_{\sqrt{M}}^d$ within the axis cross $\mathrm{X}_{\sqrt{M}}^d$ such that $\mathrm{e}^{2\pi \mathrm{i} \boldsymbol{k}^1 \cdot \boldsymbol{x}_j} = \mathrm{e}^{2\pi \mathrm{i} \boldsymbol{k}^2 \cdot \boldsymbol{x}_j}$ for all $j = 0, \ldots, M-1$.

Proof. First, we assume

$$\sum_{j=0}^{M-1} \mathrm{e}^{2\pi \mathrm{i} \boldsymbol{h} \cdot \boldsymbol{x}_j} = 0 \text{ for all } \boldsymbol{h} \in P_{\sqrt{M}}^d \setminus \{\boldsymbol{0}\}, \tag{3.1}$$

cf. Figure 3.1b for an illustration of the index set. Consequently, for all $\boldsymbol{h}^1, \boldsymbol{h}^2 \in \tilde{P}_{\sqrt{M}}^d := \{0, \ldots, \left\lfloor \sqrt{M} \right\rfloor\}^2 \times \underbrace{\{0\} \times \ldots \times \{0\}}_{d-2 \text{ times}}$ we achieve $\boldsymbol{h}^2 - \boldsymbol{h}^1 \in P_{\sqrt{M}}^d$ and

$$\sum_{j=0}^{M-1} \mathrm{e}^{2\pi \mathrm{i} (\boldsymbol{h}^2 - \boldsymbol{h}^1) \cdot \boldsymbol{x}_j} = \begin{cases} M & : \ \boldsymbol{h}^2 - \boldsymbol{h}^1 = 0 \\ 0 & \text{otherwise.} \end{cases}$$

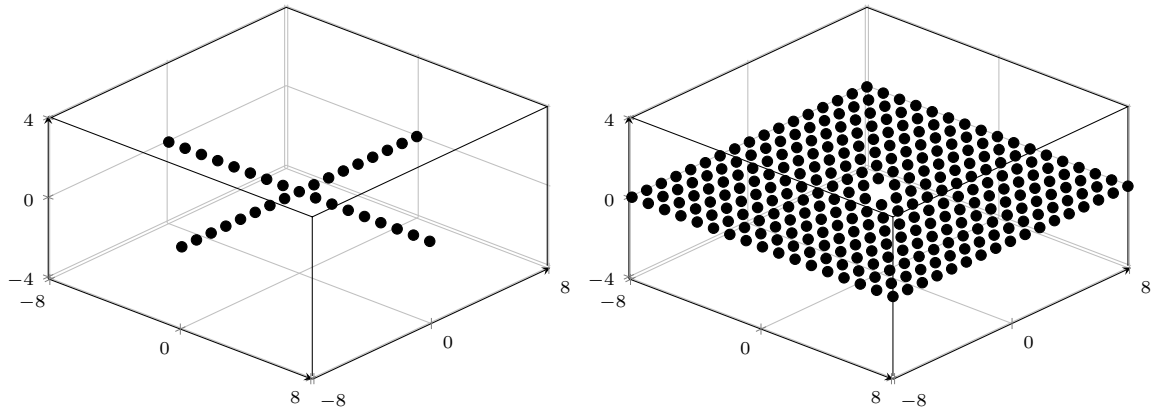

(a) X_8^3 (b) $P_8^2 \setminus \{\mathbf{0}\}$

Figure 3.1: Axis cross and subset of the difference set of the corresponding axis cross.

In matrix vector notation this means

$$\boldsymbol{A}^* \boldsymbol{A} = M \boldsymbol{I},$$

where the matrix $\boldsymbol{A} = \left(\mathrm{e}^{2\pi \mathrm{i} \boldsymbol{h} \cdot \boldsymbol{x}_j}\right)_{j=0,\ldots,M-1,\, \boldsymbol{h} \in \tilde{P}^d_{\sqrt{M}}} \in \mathbb{C}^{M \times \left(\lfloor \sqrt{M} \rfloor + 1\right)^2}$ must have full column rank. However, this is not possible due to the inequality $M < \left(\left\lfloor \sqrt{M} \right\rfloor + 1\right)^2$. Thus, the assumption given in (3.1) does not hold in any case.
Accordingly, we consider the case where $\sum_{j=0}^{M-1} \mathrm{e}^{2\pi \mathrm{i} \boldsymbol{h'} \cdot \boldsymbol{x}_j} = M$ for at least one $\boldsymbol{h'} \in P^d_{\sqrt{M}} \setminus \{\mathbf{0}\}$. Consequently, we observe $\mathrm{e}^{2\pi \mathrm{i} \boldsymbol{h'} \cdot \boldsymbol{x}_j} = 1$ for all $j = 0, \ldots, M-1$. Then, for the frequency indices $\boldsymbol{k}^1 = (h'_1, 0 \ldots, 0)^\top \in \mathrm{X}^d_{\sqrt{M}}$ and $\boldsymbol{k}^2 = (0, -h'_2, 0 \ldots, 0)^\top \in \mathrm{X}^d_{\sqrt{M}}$, the equalities $\mathrm{e}^{2\pi \mathrm{i} \boldsymbol{k}^1 \cdot \boldsymbol{x}_j} = \mathrm{e}^{2\pi \mathrm{i} \boldsymbol{k}^2 \cdot \boldsymbol{x}_j}$, $j = 0, \ldots, M-1$, hold. ■

As a consequence of the last considerations, we know that for each d-dimensional rank-1 lattice of size M, $d \geq 2$, there is at least one pair $\boldsymbol{k}^1, \boldsymbol{k}^2 \in \mathrm{X}^d_{\lfloor \sqrt{M} \rfloor} = \mathrm{X}^d_{\sqrt{M}}$ of frequencies within the two-dimensional axis cross of size $\sqrt{M}$ fulfilling

$$\boldsymbol{k}^1 \cdot \boldsymbol{z} \equiv \boldsymbol{k}^2 \cdot z \pmod{M}.$$

We call such a pair aliasing pair. As a consequence, we estimate the error of rank-1 lattice sampling operators from below as follows.

Theorem 3.2. *Let the smoothness parameters $\alpha, \beta, \gamma \in \mathbb{R}$, $\alpha > \gamma - \beta \geq 0$, $\alpha + \beta > \frac{1}{2}$. Then, we obtain*

$$g_M^{\mathrm{latt}_1}(\mathcal{H}^{\alpha,\beta}(\mathbb{T}^d), \mathcal{H}^{\gamma}(\mathbb{T}^d)) \geq 2^{-(\alpha+\beta-\gamma+1)/2} M^{-(\alpha+\beta-\gamma)/2} \tag{3.2}$$

and

$$g_M^{\mathrm{latt}_1}(\mathcal{H}^{\alpha,\beta}(\mathbb{T}^d), \mathcal{H}^{\gamma}_{\mathrm{mix}}(\mathbb{T}^d)) \geq 2^{-(\alpha+\beta-\gamma+1)/2} M^{-(\alpha+\beta-\gamma)/2}. \tag{3.3}$$

for all $M \in \mathbb{N}$.

Proof. For a given rank-1 lattice $\Lambda(\boldsymbol{z}, M)$, we construct the fooling function $\tilde{g}(\boldsymbol{x}) := \mathrm{e}^{2\pi\mathrm{i}\boldsymbol{k}^1\cdot\boldsymbol{x}} - \mathrm{e}^{2\pi\mathrm{i}\boldsymbol{k}^2\cdot\boldsymbol{x}}$, where $\boldsymbol{k}^1, \boldsymbol{k}^2 \in \mathrm{X}^d_{\sqrt{M}}$ are aliasing frequency indices with respect to $\Lambda(\boldsymbol{z}, M)$, i.e., $\boldsymbol{k}^1 \cdot \boldsymbol{z} \equiv \boldsymbol{k}^2 \cdot \boldsymbol{z} \pmod{M}$. These aliasing frequency indices exist due to Lemma 3.1. Using the notation

$$\omega^{d,\alpha,\beta}(\boldsymbol{k})^2 := \Big[\prod_{s=1}^{d}(1+|k_s|^2)\Big]^{\alpha}(1+\|\boldsymbol{k}\|_2^2)^{\beta},$$

the normalization of $\tilde{g}$ in $\mathcal{H}^{\alpha,\beta}(\mathbb{T})$ is given by

$$g(x) := \frac{\mathrm{e}^{2\pi\mathrm{i}\boldsymbol{k}^1\cdot\boldsymbol{x}} - \mathrm{e}^{2\pi\mathrm{i}\boldsymbol{k}^2\cdot\boldsymbol{x}}}{\sqrt{\omega^{d,\alpha,\beta}(\boldsymbol{k}^1)^2 + \omega^{d,\alpha,\beta}(\boldsymbol{k}^2)^2}}.$$

According to Lemma 3.1, the fooling function g is zero at all sampling nodes $\boldsymbol{x}_j \in \Lambda(\boldsymbol{z}, M)$ and we obtain

$$\|g|\mathcal{H}^{\gamma}(\mathbb{T}^d)\| = \frac{\sqrt{\omega^{d,0,\gamma}(\boldsymbol{k}^1)^2 + \omega^{d,0,\gamma}(\boldsymbol{k}^2)^2}}{\sqrt{\omega^{d,\alpha,\beta}(\boldsymbol{k}^1)^2 + \omega^{d,\alpha,\beta}(\boldsymbol{k}^2)^2}}.$$

W.l.o.g. we assume $\|\boldsymbol{k}^1\|_\infty \geq \|\boldsymbol{k}^2\|_\infty$, i.e., $\omega^{d,0,\gamma}(\boldsymbol{k}^1) \geq \omega^{d,0,\gamma}(\boldsymbol{k}^2)$ and $\omega^{d,\alpha,\beta}(\boldsymbol{k}^1) \geq \omega^{d,\alpha,\beta}(\boldsymbol{k}^2)$. We achieve

$$\|g|\mathcal{H}^{\gamma}(\mathbb{T}^d)\| \geq \frac{\sqrt{\omega^{d,0,\gamma}(\boldsymbol{k}^1)^2}}{\sqrt{2\omega^{d,\alpha,\beta}(\boldsymbol{k}^1)^2}} = \frac{1}{\sqrt{2}\omega^{d,\alpha,\beta-\gamma}(\boldsymbol{k}^1)}. \tag{3.4}$$

For $\boldsymbol{k} \in \mathrm{X}^d_{\sqrt{M}}$ with $|k_1| = \|\boldsymbol{k}\|_\infty$ and $M \in \mathbb{N}$ we have

$$\begin{aligned}\omega^{d,\alpha,\beta-\gamma}(\boldsymbol{k}) &= (1+|k_1|^2)^{(\alpha+\beta-\gamma)/2} \\ &\leq (1+M)^{(\alpha+\beta-\gamma)/2} \leq (2M)^{(\alpha+\beta-\gamma)/2}.\end{aligned}$$

Inserting this into (3.4) yields

$$\|g|\mathcal{H}^{\gamma}(\mathbb{T}^d)\| \geq 2^{-(\alpha+\beta-\gamma+1)/2} M^{-(\alpha+\beta-\gamma)/2}$$

Now (3.2) follows by a standard argument. Let $A : \mathbb{C}^M \mapsto \mathcal{H}^{\gamma}(\mathbb{T}^d)$ be an arbitrary algorithm applied to $\left(f(\boldsymbol{0}), f\left(\frac{1}{M}\boldsymbol{z}\right), \ldots, f\left(\frac{M-1}{M}\boldsymbol{z}\right)\right) = \boldsymbol{0}$. We estimate as follows

$$\begin{aligned}2^{-(\alpha+\beta-\gamma+1)/2} M^{-(\alpha+\beta-\gamma)/2} &\leq \|g|\mathcal{H}^{\gamma}(\mathbb{T})\| \leq \frac{1}{2}(\|g - A(\boldsymbol{0})|\mathcal{H}^{\gamma}(\mathbb{T})\| + \|-g - A(\boldsymbol{0})|\mathcal{H}^{\gamma}(\mathbb{T}))\| \\ &\leq \max\{\|g - A(\boldsymbol{0})|\mathcal{H}^{\gamma}(\mathbb{T})\|, \|-g - A(\boldsymbol{0})|\mathcal{H}^{\gamma}(\mathbb{T})\|\}.\end{aligned}$$

Accordingly, each algorithm A badly approximates at least one of the functions g or $-g$. Thus, we observe an infimum over the worst case errors of all algorithms A

$$\mathrm{Samp}_{\Lambda(\boldsymbol{z},M)}(\mathcal{H}^{\alpha,\beta}(\mathbb{T}^d), H^{\gamma}(\mathbb{T}^d)) \geq 2^{-(\alpha+\beta-\gamma+1)/2} M^{-(\alpha+\beta-\gamma)/2}.$$

Finally the infimum over all rank-1 lattices with M points yields

$$\mathrm{g}^{\mathrm{latt}_1}_M(\mathcal{H}^{\alpha,\beta}(\mathbb{T}^d), H^{\gamma}(\mathbb{T}^d)) \geq 2^{-(\alpha+\beta-\gamma+1)/2} M^{-(\alpha+\beta-\gamma)/2}.$$

The assertion in (3.3) can be proven analogously. ∎

Following attentively the last proof we recognize that the condition $\alpha + \beta > \frac{1}{2}$ plays no fundamental role in the estimations there. It is required for a well interpretation of the function evaluations in the definition of $g_M^{\mathrm{latt}_1}(\mathcal{H}^{\alpha,\beta}(\mathbb{T}^d), Y)$, which is given for continuous functions (cf. Lemma 2.1). For $\min\{\alpha, \alpha+\beta\} > 0$, a generalization of the last theorem can be achieved using the space

$$\mathcal{H}^{\alpha,\beta}(\mathbb{T}^d) \cap^* C(\mathbb{T}^d) := \left\{ f \in C(\mathbb{T}^d) \colon \|f|\mathcal{H}^{\alpha,\beta}(\mathbb{T}^d)\| < \infty \right\},$$

equipped with the norm of $\mathcal{H}^{\alpha,\beta}(\mathbb{T}^d)$, see (2.1) for comparison. Then the proof of Theorem 3.2 yields the following proposition.

Proposition 3.3. Let the smoothness parameters $\alpha, \beta, \gamma \in \mathbb{R}$, $\alpha > \gamma - \beta \geq 0$, $\alpha + \beta > 0$. Then, we obtain

$$g_M^{\mathrm{latt}_1}(\mathcal{H}^{\alpha,\beta}(\mathbb{T}^d) \cap^* C(\mathbb{T}^d), \mathcal{H}^{\gamma}(\mathbb{T}^d)) \geq 2^{-(\alpha+\beta-\gamma+1)/2} M^{-(\alpha+\beta-\gamma)/2}$$

and

$$g_M^{\mathrm{latt}_1}(\mathcal{H}^{\alpha,\beta}(\mathbb{T}^d) \cap^* C(\mathbb{T}^d), \mathcal{H}^{\gamma}_{\mathrm{mix}}(\mathbb{T}^d)) \geq 2^{-(\alpha+\beta-\gamma+1)/2} M^{-(\alpha+\beta-\gamma)/2}.$$

for all $M \in \mathbb{N}$.

Remark 3.4. We stress on the fact that even each d-dimensional rank-s lattice of size M, where $d \geq 2$ and $s \in \mathbb{N}$, $s \leq d$, fulfills the requirements of Lemma 3.1, cf. [35, Lemma 2.7]. Consequently, there exists at least one aliasing pair $\boldsymbol{k}^1, \boldsymbol{k}^2 \in \mathrm{X}^d_{\sqrt{M}}$ within the two-dimensional axis cross of size $\sqrt{M}$. This means we obtain the statements of Theorem 3.2 using the identical proof strategy.

4 Improved upper bounds for $d > 2$

In this section we study upper bounds for $g_M^{\mathrm{latt}_1}$. To do this, we consider approximation error estimates for $S^{\Lambda(\boldsymbol{z},M)}_{H^{d,T}_R} f$. To obtain these estimates the cardinality of the dual lattice $\Lambda(\boldsymbol{z}, M)^\perp$ intersected with rectangular boxes Ω plays an important role.

Lemma 4.1. *Let $\Lambda(\boldsymbol{z}, M)$ be a rank-1 lattice generated by $\boldsymbol{z} \in \mathbb{Z}^d$ with M points. Assume that the dual lattice $\Lambda(\boldsymbol{z}, M)^\perp$ is located outside the hyperbolic cross $H^{d,0}_R$, $R \geq 1$, i.e.,*

$$\Lambda(\boldsymbol{z}, M)^\perp \cap H^{d,0}_R = \{\boldsymbol{0}\}. \tag{4.1}$$

Then we have

$$|\Lambda(\boldsymbol{z}, M)^\perp \cap \Omega| \leq \begin{cases} 2^{d+1} \frac{\mathrm{vol}\,\Omega}{2^R} & : \mathrm{vol}\,\Omega > 2^{R-1}, \\ 1 & : \mathrm{vol}\,\Omega \leq 2^{R-1}, \end{cases} \tag{4.2}$$

where Ω is an arbitrary rectangle with side-lenghts ≥ 1.

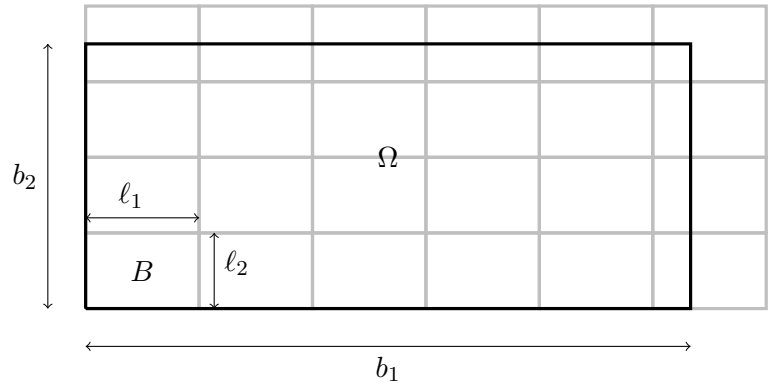

Figure 4.1: The counting argument in Lemma 4.1.

Proof. For two arbitrary distinct dual lattice points $\boldsymbol{k}^1, \boldsymbol{k}^2 \in \Lambda(\boldsymbol{z}, M)^\perp$, $\boldsymbol{k}^1 \neq \boldsymbol{k}^2$, we obtain $\boldsymbol{k} := \boldsymbol{k}^1 - \boldsymbol{k}^2 \in \Lambda(\boldsymbol{z}, M)^\perp \setminus \{\boldsymbol{0}\}$. As a consequence of (2.8) and (4.1), the vector $\boldsymbol{k}$ belongs to a cuboid $Q_{\boldsymbol{j}}$ with $\|\boldsymbol{j}\|_1 > R + d - 1$. We achieve

$$\prod_{s=1}^{d} \max\{|k_s|, 1\} = \prod_{\substack{s=1 \\ j_s>0}}^{d} |k_s| \geq \prod_{\substack{s=1 \\ j_s>0}}^{d} (2^{j_s-1} + 1) > \prod_{\substack{s=1 \\ j_s>0}}^{d} 2^{j_s-1} \geq 2^{\|\boldsymbol{j}\|_1 - d} > 2^{R-1}.$$

Step 1. We prove the second case in (4.2) by contradiction. For any rectangle $\Omega := [a_1, a_1+b_1]\times\ldots\times[a_d, a_d+b_d]$ with side lengths $b_s \geq 1$, $s = 1, \ldots, d$, and $\operatorname{vol}\Omega = \prod_{s=1}^{d} b_s \leq 2^{R-1}$ we assume $|\Lambda(\boldsymbol{z}, M)^\perp \cap \Omega| \geq 2$ and we choose $\boldsymbol{k}^1, \boldsymbol{k}^2 \in \Omega \cap \Lambda(\boldsymbol{z}, M)^\perp$, $\boldsymbol{k}^1 \neq \boldsymbol{k}^2$. Consequently, there is a d-dimensional cuboid $K \subset \Omega$ of side lengths ≥ 1 which contains the minimal cuboid with edges $\boldsymbol{k}^1$ and $\boldsymbol{k}^2$. The volume of K is bounded from below by $\prod_{s=1}^{d} \max\{|k_s|, 1\} > 2^{R-1}$, and hence larger than the volume of Ω, which is in contradiction to the relation $K \subset \Omega$. Accordingly, there can not be more than one element within $\Lambda(\boldsymbol{z}, M)^\perp \cap \Omega$.

Step 2. We prove the first case and assume that Ω has volume larger than 2^{R-1}. The sidelengths of Ω are denoted by b_s, $s = 1, \ldots, d$. We construct a disjoint covering/packing of Ω consisting of half side opened cuboids B with sidelength $\ell_1, \ldots, \ell_d$ such that $\ell_s \leq \max(1, b_s)$, $s = 1, \ldots, d$, and $\operatorname{vol} B = 2^{R-1}$, cf. Figure 4.1 for illustration. We need at most $2^d \frac{\operatorname{vol}\Omega}{2^{R-1}}$ of the cuboids B in order to cover the set Ω. Due to Step 1, each B contains at most one element from $\Lambda(\boldsymbol{z}, M)^\perp$. Accordingly, the number of elements in $\Lambda(\boldsymbol{z}, M)^\perp \cap \Omega$ is bounded from above by $2^{d+1} \frac{\operatorname{vol}\Omega}{2^R}$. ∎

Lemma 4.2. *Let the smoothness parameters $\alpha, \beta \in \mathbb{R}$, $\beta \leq 0$, $\alpha + \beta > 1/2$, the refinement $R \geq 1$, and the parameter $T := -\beta/\alpha$ be given. In addition, we assume that the rank-1 lattice $\Lambda(\boldsymbol{z}, M)$ is a reconstructing rank-1 lattice for the hyperbolic cross $H_R^{d,0}$. We define*

$$\theta_{\alpha,\beta}^2(\boldsymbol{k}, \boldsymbol{z}, M) := \sum_{\substack{\boldsymbol{h}\in\Lambda(\boldsymbol{z},M)^\perp \\ \boldsymbol{h}\neq\boldsymbol{0}}} (1 + \|\boldsymbol{k} + \boldsymbol{h}\|_2^2)^{-\beta} \prod_{s=1}^{d} (1 + |k_s + h_s|^2)^{-\alpha}. \tag{4.3}$$

Then the estimate

$$\theta_{\alpha,\beta}^2(\boldsymbol{k}, \boldsymbol{z}, M) \lesssim \begin{cases} 2^{-2(\alpha+\beta)R} & : \ T > 0, \\ 2^{-2\alpha R} R^{d-1} & : \ T = \beta = 0 \end{cases}$$

holds for all $\boldsymbol{k} \in H_R^{d,0}$.

Proof. For $\boldsymbol{k} \in \mathbb{Z}^d$ and $\boldsymbol{j} \in \mathbb{N}_0^d$ we define the indicator function

$$\varphi_{\boldsymbol{j}}(\boldsymbol{k}) := \begin{cases} 0 & : \ \boldsymbol{k} \notin Q_{\boldsymbol{j}}, \\ 1 & : \ \boldsymbol{k} \in Q_{\boldsymbol{j}}, \end{cases}$$

where $Q_{\boldsymbol{j}}$ is defined in (2.9). We fix $\boldsymbol{k} \in H_R^{d,0}$ and decompose the sum in (4.3), which yields

$$\theta_{\alpha,\beta}^2(\boldsymbol{k}, \boldsymbol{z}, M) = \sum_{\substack{\boldsymbol{h} \in \Lambda(\boldsymbol{z},M)^\perp \\ \boldsymbol{h} \neq \boldsymbol{0}}} \sum_{\boldsymbol{j} \in \mathbb{N}_0^d} \varphi_{\boldsymbol{j}}(\boldsymbol{k}+\boldsymbol{h})(1+\|\boldsymbol{k}+\boldsymbol{h}\|_2^2)^{-\beta} \prod_{s=1}^{d} (1+|k_s+h_s|^2)^{-\alpha}.$$

Since $\Lambda(\boldsymbol{z}, M)$ is a reconstructing rank-1 lattice for $H_R^{d,0}$, we know from (2.7) that

$$\mathcal{D}(H_R^{d,0}) \cap \Big(\Lambda(\boldsymbol{z}, M)^\perp \setminus \{\boldsymbol{0}\} \Big) = \emptyset \,.$$

This yields

$$\boldsymbol{k}^1 + \boldsymbol{h}^1 \neq \boldsymbol{k}^2 + \boldsymbol{h}^2$$

for all $\boldsymbol{k}^1, \boldsymbol{k}^2 \in H_R^{d,0}$, $\boldsymbol{k}^1 \neq \boldsymbol{k}^2$, and $\boldsymbol{h}^1, \boldsymbol{h}^2 \in \Lambda(\boldsymbol{z}, M)^\perp$ since otherwise $\boldsymbol{0} \neq \boldsymbol{k}^1 - \boldsymbol{k}^2 = \boldsymbol{h}^2 - \boldsymbol{h}^1 \in \Lambda(\boldsymbol{z}, M)^\perp$ which is in contradiction to (2.7). In particular, we have that $\boldsymbol{k} + \boldsymbol{h} \notin H_R^{d,0}$ for all $\boldsymbol{k} \in H_R^{d,0}$ and $\boldsymbol{h} \in \Lambda(\boldsymbol{z}, M)^\perp \setminus \{\boldsymbol{0}\}$. Accordingly, we modify the summation index set for $\boldsymbol{j}$ and we estimate the summands

$$\theta_{\alpha,\beta}^2(\boldsymbol{k}, \boldsymbol{z}, M) \lesssim \sum_{\boldsymbol{j} \in \mathbb{N}_0^d \setminus J_R^{d,0}} 2^{-2(\alpha\|\boldsymbol{j}\|_1 + \beta\|\boldsymbol{j}\|_\infty)} \sum_{\substack{\boldsymbol{h} \in \Lambda(\boldsymbol{z},M)^\perp \\ \boldsymbol{h} \neq \boldsymbol{0}}} \varphi_{\boldsymbol{j}}(\boldsymbol{k}+\boldsymbol{h}).$$

We apply Lemma 4.1 and get

$$\theta_{\alpha,\beta}^2(\boldsymbol{k}, \boldsymbol{z}, M) \lesssim 2^{-R} \sum_{\boldsymbol{j} \in \mathbb{N}_0^d \setminus J_R^{d,0}} 2^{-((2\alpha-1)\|\boldsymbol{j}\|_1 + \beta\|\boldsymbol{j}\|_\infty)}.$$

Taking Lemma 4.3 into account, the assertion follows. ∎

Lemma 4.3. *Let the smoothness parameters* $\alpha, \beta \in \mathbb{R}$, $\beta \leq 0$, $\alpha+\beta > 1/2$, *and the refinement* $R \geq 1$ *be given. Then, we estimate*

$$\sum_{\boldsymbol{j} \in \mathbb{N}_0^d \setminus J_R^{d,T}} 2^{-((2\alpha-1)\|\boldsymbol{j}\|_1 + 2\beta\|\boldsymbol{j}\|_\infty)} \lesssim \begin{cases} 2^{-(2\alpha-1+2\beta)R} & : \ T \leq -\frac{\beta}{\alpha} \text{ and } \beta < 0, \\ 2^{-(2\alpha-1)R} R^{d-1} & : \ T = \beta = 0. \end{cases}$$

Proof. In the proof of [20, Theorem 4] one finds the following estimate

$$\sum_{\boldsymbol{j} \in \mathbb{N}_0^d \setminus J_R^{d,T}} 2^{-t\|\boldsymbol{j}\|_1 + s\|\boldsymbol{j}\|_\infty} \lesssim \begin{cases} 2^{(s-t)R} & : \ T < \frac{s}{t}, \\ R^{d-1} 2^{(s-t+(Tt-s)\frac{d-1}{d-T})R} & : \ T \geq \frac{s}{t} \end{cases}$$

for $s < t$ and $t \geq 0$. Accordingly, we apply this result setting $s := -2\beta$ and $t := 2\alpha - 1$. We require $\beta \leq 0$ and obtain the necessity $\alpha + \beta > 1/2$ from the conditions $s < t$ and $t \geq 0$. Moreover, we set the parameter $T := -\beta/\alpha$. This yields

$$T = \frac{s}{t+1} \begin{cases} = 0 & : \ 0 = s = \beta, \\ < \frac{s}{t} & : \ 0 < s = -2\beta. \end{cases}$$

Consequently, we achieve the assertion. ∎

Theorem 4.4. *Let the smoothness parameters $\alpha > \frac{1}{2}$, $\beta \leq 0$, $\gamma \geq 0$ with $\alpha + \beta > \max\{\gamma, \frac{1}{2}\}$, the dimension $d \in \mathbb{N}$, $d \geq 2$, and the refinement $R \geq 1$, be given. In addition, we assume that $\Lambda(\boldsymbol{z}, M)$ is a reconstructing rank-1 lattice for $H_R^{d,0}$. We estimate the error of the sampling operator $\mathrm{Id} - S_{H_R^{d,0}}^{\Lambda(\boldsymbol{z},M)}$ by*

$$M^{-(\alpha+\beta-\gamma)/2} \lesssim \|\mathrm{Id} - S_{H_R^{d,0}}^{\Lambda(\boldsymbol{z},M)} | \mathcal{H}^{\alpha,\beta}(\mathbb{T}^d) \to \mathcal{H}^{\gamma}_{\mathrm{mix}}(\mathbb{T}^d)\| \lesssim 2^{-(\alpha+\beta-\gamma)R} \begin{cases} R^{(d-1)/2} & : \ \beta = 0, \\ 1 & : \ \beta < 0. \end{cases}$$

If $\Lambda(\boldsymbol{z}, M)$ is constructed by the CBC strategy [14, Tab. 3.1] we continue

$$\lesssim M^{-(\alpha+\beta-\gamma)/2} (\log M)^{\frac{d-2}{2}(\alpha+\beta-\gamma)} \begin{cases} (\log M)^{(d-1)/2} & : \ \beta = 0, \\ 1 & : \ \beta < 0. \end{cases}$$

Proof. The lower bound was discussed in Theorem 3.2. We apply the triangle inequality and split up the error of the sampling operator into the error of the best approximation and the aliasing error. The error of the projection operator $S_{H_R^{d,0}}$ can be easily estimated using

$$\begin{aligned} \|f - S_{H_R^{d,0}} f | \mathcal{H}^{\gamma}_{\mathrm{mix}}(\mathbb{T}^d)\| &= \Big(\sum_{\boldsymbol{k} \notin H_R^{d,0}} (1 + \|\boldsymbol{k}\|_2^2)^{\gamma} |\hat{f}_{\boldsymbol{k}}|^2 \Big)^{\frac{1}{2}} \\ &\leq \sup_{k \notin H_R^{d,0}} \Big(\frac{1}{(1 + \|\boldsymbol{k}\|_2^2)^{\beta} \prod_{s=1}^{d} (1 + |k_s|^2)^{\alpha-\gamma}} \Big)^{\frac{1}{2}} \\ &\quad \Big(\sum_{\boldsymbol{k} \notin H_R^{d,0}} (1 + \|\boldsymbol{k}\|_2^2)^{\beta} \Big[\prod_{s=1}^{d} (1 + |k_s|^2)^{\alpha} \Big] |\hat{f}_{\boldsymbol{k}}|^2 \Big)^{\frac{1}{2}}. \end{aligned} \tag{4.4}$$

It is easy to check that (4.4) becomes maximal at the peaks of the hyperbolic cross. Therefore we obtain

$$\|f - S_{H_R^{d,0}} f | \mathcal{H}^{\gamma}_{\mathrm{mix}}(\mathbb{T}^d)\| \lesssim 2^{-(\alpha+\beta-\gamma)R} \|f | \mathcal{H}^{\alpha,\beta}(\mathbb{T}^d)\|.$$

The aliasing error fulfills

$$\|S_{H_R^{d,0}} f - S_{H_R^{d,0}}^{\Lambda(\boldsymbol{z},M)} f | \mathcal{H}^{\gamma}_{\mathrm{mix}}(\mathbb{T}^d)\|^2 = \sum_{\boldsymbol{k} \in H_R^{d,0}} \Big[\prod_{s=1}^{d} (1 + |k_s|^2)^{\gamma} \Big] \Big| \sum_{\substack{\boldsymbol{h} \in \Lambda(\boldsymbol{z},M)^{\perp} \\ \boldsymbol{h} \neq \boldsymbol{0}}} \hat{f}_{\boldsymbol{k}+\boldsymbol{h}} \Big|^2$$

Applying Hölder's inequality twice yields

$$
\begin{aligned}
&\|S_{H_R^{d,0}} f - S^{\Lambda(\boldsymbol{z},M)}_{H_R^{d,0}} f|\mathcal{H}^\gamma_{\mathrm{mix}}(\mathbb{T}^d)\|^2 \\
&\quad\le \sum_{\boldsymbol{k}\in H_R^{d,0}} \Big[\prod_{s=1}^d (1+|k_s|^2)^\gamma\Big] \Big(\underbrace{\sum_{\substack{\boldsymbol{h}\in\Lambda(\boldsymbol{z},M)^\perp\\ \boldsymbol{h}\neq\boldsymbol{0}}} (1+\|\boldsymbol{k}+\boldsymbol{h}\|_2^2)^{-\beta} \prod_{s=1}^d (1+|k_s+h_s|^2)^{-\alpha}}_{=:\theta^2_{\alpha,\beta}(\boldsymbol{k},\boldsymbol{z},M),\ \text{cf. (4.3)}} \Big). \\
&\quad \Big(\sum_{\substack{\boldsymbol{h}\in\Lambda(\boldsymbol{z},M)^\perp\\ \boldsymbol{h}\neq\boldsymbol{0}}} (1+\|\boldsymbol{k}+\boldsymbol{h}\|_2^2)^{\beta} \Big[\prod_{s=1}^d (1+|k_s+h_s|^2)^{\alpha}\Big] |\hat{f}_{\boldsymbol{k}+\boldsymbol{h}}|^2 \Big) \\
&\quad\le \sup_{\boldsymbol{k}\in H_R^{d,0}} \Big[\prod_{s=1}^d (1+|k_s|^2)^\gamma\Big] \theta^2_{\alpha,\beta}(\boldsymbol{k},\boldsymbol{z},M) \\
&\quad \Big(\sum_{\boldsymbol{k}\in H_R^{d,0}} \sum_{\substack{\boldsymbol{h}\in\Lambda(\boldsymbol{z},M)^\perp\\ \boldsymbol{h}\neq\boldsymbol{0}}} (1+\|\boldsymbol{k}+\boldsymbol{h}\|_2^2)^{\beta} \Big[\prod_{s=1}^d (1+|k_s+h_s|^2)^{\alpha}\Big] |\hat{f}_{\boldsymbol{k}+\boldsymbol{h}}|^2 \Big) \\
&\quad\le \sup_{\boldsymbol{h}\in H_R^{d,0}} \Big[\prod_{s=1}^d (1+|h_s|^2)^\gamma\Big] \sup_{\boldsymbol{k}\in H_R^{d,0}} \theta^2_{\alpha,\beta}(\boldsymbol{k},\boldsymbol{z},M) \|f|\mathcal{H}^{\alpha,\beta}(\mathbb{T}^d)\|^2 \qquad (4.5)
\end{aligned}
$$

since $\Lambda(\boldsymbol{z},M)$ is a reconstructing rank-1 lattice for $H_R^{d,0}$ and, consequently, the sets $\{\boldsymbol{k}+\boldsymbol{h}\in\mathbb{Z}^d\colon \boldsymbol{h}\in\Lambda(\boldsymbol{z},M)^\perp\}$, $\boldsymbol{k}\in H_R^{d,0}$, do not intersect. We apply Lemma 4.2 and take the upper bound

$$
\sup_{\boldsymbol{k}\in H_R^{d,0}} \prod_{s=1}^d (1+|k_s|^2)^\gamma \lesssim \sup_{\boldsymbol{j}\in J_R^{d,0}} 2^{2\gamma\|\boldsymbol{j}\|_1} \lesssim 2^{2\gamma R}
$$

into account. We achieve

$$
\|S_{H_R^{d,0}} f - S^{\Lambda(\boldsymbol{z},M)}_{H_R^{d,0}} f|\mathcal{H}^\gamma_{\mathrm{mix}}(\mathbb{T}^d)\| \lesssim \|f|\mathcal{H}^{\alpha,\beta}(\mathbb{T}^d)\|\, 2^{-(\alpha+\beta-\gamma)R} \begin{cases} R^{\frac{d-1}{2}} & :\ \beta=0, \\ 1 & :\ \beta<0 \end{cases}
$$

and, in conjunction with Lemma 2.3, the second assertion of the theorem. ∎

Remark 4.5. The basic improvement in the error analysis compared to [19] is provided by applying Lemma 4.1 in (4.5). Here, the information about the cardinality of the dual lattice intersected with rectangular boxes yields sharp main rates coinciding with the lower bounds given in Theorem 3.2. From that viewpoint this technique improves also the asymptotical main rates obtained in [25] for the $L_2(\mathbb{T}^d)$ approximation error. In case $\beta<0$ and $\gamma=0$ the result above behaves not optimal compared to the result obtained in [19] where a Korobov type lattice is used. The authors there obtain no logarithmic dependence in M. The main reason for that issue is the probably technical limitation in Lemma 4.1 discussed in Remark 6.3 that does not allow us to use energy-type hyperbolic crosses as index sets, here.

Due to the embedding $\mathcal{H}^\gamma_{\mathrm{mix}}(\mathbb{T}^d)\hookrightarrow\mathcal{H}^\gamma(\mathbb{T}^d)$ we obtain the following proposition.

Proposition 4.6. Let the smoothness parameters $\alpha > \frac{1}{2}$, $\beta \leq 0$, $\gamma \geq 0$ with $\alpha + \beta > \max\{\gamma, \frac{1}{2}\}$, the dimension $d \in \mathbb{N}$, $d \geq 2$, and the refinement $R \geq 1$, be given. In addition, we assume that $\Lambda(\boldsymbol{z}, M)$ is a reconstructing rank-1 lattice for $H_R^{d,0}$ constructed by the CBC strategy [14, Tab. 3.1]. We estimate the error of the sampling operator $\mathrm{Id} - S_{H_R^{d,0}}^{\Lambda(\boldsymbol{z},M)}$ by

$$\begin{aligned} M^{-(\alpha+\beta-\gamma)/2} &\lesssim \|\mathrm{Id} - S_{H_R^{d,0}}^{\Lambda(\boldsymbol{z},M)} | \mathcal{H}^{\alpha,\beta}(\mathbb{T}^d) \to \mathcal{H}^{\gamma}(\mathbb{T}^d)\| \lesssim 2^{-(\alpha+\beta-\gamma)R} \begin{cases} R^{(d-1)/2} & : \ \beta = 0, \\ 1 & : \ \beta < 0 \end{cases} \\ &\lesssim M^{-(\alpha+\beta-\gamma)/2} (\log M)^{(d-2)(\alpha+\beta-\gamma)/2} \begin{cases} (\log M)^{(d-1)/2} & : \ \beta = 0, \\ 1 & : \ \beta < 0. \end{cases} \end{aligned}$$

■

For $2 < q < \infty$ the embedding

$$\mathcal{H}^{\frac{1}{2}-\frac{1}{q}}(\mathbb{T}^d) \hookrightarrow L_q(\mathbb{T}^d)$$

(see [30], 2.4.1) extends the last theorem to target spaces $L_q(\mathbb{T}^d)$.

Proposition 4.7. Let the smoothness parameters $\alpha > \frac{1}{2}$ and $\beta \leq 0$ with $\alpha + \beta > \frac{1}{2}$, $2 < q < \infty$. Let the dimension $d \in \mathbb{N}$, $d \geq 2$, and the refinement $R \geq 1$, be given. In addition, we assume that $\Lambda(\boldsymbol{z}, M)$ is a reconstructing rank-1 lattice for $H_R^{d,0}$ constructed by the CBC strategy [14, Tab. 3.1]. We estimate the error of the sampling operator $\mathrm{Id} - S_{H_R^{d,0}}^{\Lambda(\boldsymbol{z},M)}$ by

$$\begin{aligned} \|\mathrm{Id} - S_{H_R^{d,0}}^{\Lambda(\boldsymbol{z},M)} | \mathcal{H}^{\alpha,\beta}(\mathbb{T}^d) \to L_q(\mathbb{T}^d)\| &\lesssim 2^{-(\alpha+\beta-(\frac{1}{2}-\frac{1}{q}))R} \begin{cases} R^{(d-1)/2} & : \ \beta = 0, \\ 1 & : \ \beta < 0 \end{cases} \\ &\lesssim M^{-(\alpha+\beta-(\frac{1}{2}-\frac{1}{q}))/2} (\log M)^{\frac{d-2}{2}(\alpha+\beta-(\frac{1}{2}-\frac{1}{q}))} \begin{cases} (\log M)^{(d-1)/2} & : \ \beta = 0, \\ 1 & : \ \beta < 0. \end{cases} \end{aligned}$$

■

In addition to $L_q(\mathbb{T}^d)$, $2 < q < \infty$, we study the case $q = \infty$. For technical reasons we estimate the sampling error with respect to the d-dimensional Wiener algebra

$$\mathcal{A}(\mathbb{T}^d) := \{f \in L_1(\mathbb{T}^d) \colon \sum_{\boldsymbol{k} \in \mathbb{Z}^d} |\hat{f}_{\boldsymbol{k}}| < \infty\}$$

and subsequently we use the embedding $\mathcal{A}(\mathbb{T}^d) \hookrightarrow C(\mathbb{T}^d) \hookrightarrow L_\infty(\mathbb{T}^d)$.

Theorem 4.8. *Let the smoothness parameters $\alpha > \frac{1}{2}$ and $\beta \leq 0$ with $\alpha + \beta > \frac{1}{2}$, the dimension $d \in \mathbb{N}$, $d \geq 2$, and the refinement $R \in \mathbb{R}$, $R \geq 1$, be given. In addition, we assume that $\Lambda(\boldsymbol{z}, M)$ is a reconstructing rank-1 lattice for $H_R^{d,T}$ with $T := -\frac{\beta}{\alpha}$ constructed by the CBC strategy [14, Tab. 3.1]. We estimate the error of the sampling operator $\mathrm{Id} - S_{H_R^{d,T}}^{\Lambda(\boldsymbol{z},M)}$ by*

$$\begin{aligned} \|\mathrm{Id} - S_{H_R^{d,T}}^{\Lambda(\boldsymbol{z},M)} | \mathcal{H}^{\alpha,\beta}(\mathbb{T}^d) \to \mathcal{A}(\mathbb{T}^d)\| &\lesssim 2^{-(\alpha+\beta-\frac{1}{2})R} \begin{cases} R^{\frac{d-1}{2}} & : \ \beta = 0, \\ 1 & : \ \beta < 0 \end{cases} \\ &\lesssim M^{-(\alpha+\beta-\frac{1}{2})/2} \begin{cases} (\log M)^{\frac{d-2}{2}(\alpha-\frac{1}{2})+\frac{d-1}{2}} & : \ \beta = 0, \\ 1 & : \ \beta < 0. \end{cases} \end{aligned}$$

Proof. Again we use the triangle inequality and split up the error of the sampling operator into the error of the truncation error and the aliasing error. The truncation error fulfills

$$\|f - S_{H_R^{d,T}} f | \mathcal{A}(\mathbb{T}^d)\| \lesssim \|f|\mathcal{H}^{\alpha,\beta}(\mathbb{T}^d)\| 2^{-(\alpha+\beta-\frac{1}{2})R} \begin{cases} R^{\frac{d-1}{2}} & : \beta = 0, \\ 1 & : \beta < 0. \end{cases} \tag{4.6}$$

For completeness we give a short proof. Applying the orthogonal projection property of $S_{H_R^{d,T}} f$ we obtain

$$\begin{aligned} \|f - S_{H_R^{d,T}} f | \mathcal{A}(\mathbb{T}^d)\| &= \sum_{\boldsymbol{k} \notin H_R^{d,T}} |\hat{f}_{\boldsymbol{k}}| \\ &\leq \Big(\sum_{\boldsymbol{k} \notin H_R^{d,T}} (1 + \|\boldsymbol{k}\|_2^2)^{-\beta} \prod_{s=1}^{d} (1 + |k_s|^2)^{-\alpha} \Big)^{\frac{1}{2}} \Big(\sum_{\boldsymbol{k} \notin H_R^{d,T}} (1 + \|\boldsymbol{k}\|_2^2)^{\beta} \Big[\prod_{s=1}^{d} (1 + |k_s|^2)^{\alpha} \Big] |\hat{f}_{\boldsymbol{k}}|^2 \Big)^{\frac{1}{2}}. \end{aligned}$$

Decomposing the first sum into dyadic blocks yields

$$\begin{aligned} \|f - S_{H_R^{d,T}} f | \mathcal{A}(\mathbb{T}^d)\| &\leq \Big(\sum_{\boldsymbol{j} \notin J_R^{d,T}} \sum_{\boldsymbol{k} \in Q_{\boldsymbol{j}}} (1 + \|\boldsymbol{k}\|_2^2)^{-\beta} \prod_{s=1}^{d} (1 + |k_s|^2)^{-\alpha} \Big)^{\frac{1}{2}} \|f|\mathcal{H}^{\alpha,\beta}(\mathbb{T}^d)\| \\ &\lesssim \Big(\sum_{\boldsymbol{j} \notin J_R^{d,T}} 2^{-2\alpha\|\boldsymbol{j}\|_1 - 2\beta\|\boldsymbol{j}\|_\infty} \sum_{\boldsymbol{k} \in Q_{\boldsymbol{j}}} 1 \Big)^{\frac{1}{2}} \|f|\mathcal{H}^{\alpha,\beta}(\mathbb{T}^d)\| \\ &\lesssim \Big(\sum_{\boldsymbol{j} \notin J_R^{d,T}} 2^{-(2\alpha-1)\|\boldsymbol{j}\|_1 - 2\beta\|\boldsymbol{j}\|_\infty} \Big)^{\frac{1}{2}} \|f|\mathcal{H}^{\alpha,\beta}(\mathbb{T}^d)\|. \end{aligned} \tag{4.7}$$

Applying Lemma 4.3 we obtain (4.6). The aliasing error behaves as follows

$$\|S_{H_R^{d,T}} f - S^{\Lambda(\boldsymbol{z},M)}_{H_R^{d,T}} f | \mathcal{A}(\mathbb{T}^d)\| = \sum_{\boldsymbol{k} \in H_R^{d,T}} \Big| \sum_{\substack{\boldsymbol{h} \in \Lambda(\boldsymbol{z},M)^\perp \\ \boldsymbol{h} \neq \boldsymbol{0}}} \hat{f}_{\boldsymbol{k}+\boldsymbol{h}} \Big|.$$

Applying Hölder's inequality twice yields

$$\begin{aligned} &\|S_{H_R^{d,T}} f - S^{\Lambda(\boldsymbol{z},M)}_{H_R^{d,T}} f | \mathcal{A}(\mathbb{T}^d)\| \\ &\leq \Big(\sum_{\boldsymbol{k} \in H_R^{d,T}} \sum_{\substack{\boldsymbol{h} \in \Lambda(\boldsymbol{z},M)^\perp \\ \boldsymbol{h} \neq \boldsymbol{0}}} (1 + \|\boldsymbol{k} + \boldsymbol{h}\|_2^2)^{-\beta} \prod_{s=1}^{d} (1 + |k_s + h_s|^2)^{-\alpha} \Big)^{\frac{1}{2}} \\ &\quad \Big(\sum_{\boldsymbol{k} \in H_R^{d,T}} \sum_{\substack{\boldsymbol{h} \in \Lambda(\boldsymbol{z},M)^\perp \\ \boldsymbol{h} \neq \boldsymbol{0}}} (1 + \|\boldsymbol{k} + \boldsymbol{h}\|_2^2)^{\beta} \prod_{s=1}^{d} (1 + |k_s + h_s|^2)^{\alpha} |\hat{f}_{\boldsymbol{k}+\boldsymbol{h}}|^2 \Big)^{\frac{1}{2}}. \end{aligned}$$

Since $\Lambda(\boldsymbol{z}, M)$ is a reconstructing rank-1 lattice for $H_R^{d,T}$ and, consequently, the sets

$\{\boldsymbol{k}+\boldsymbol{h}\in\mathbb{Z}^d\colon \boldsymbol{h}\in\Lambda(\boldsymbol{z},M)^\perp\}$, $\boldsymbol{k}\in H_R^{d,T}$, do not intersect, we obtain

$$\begin{aligned}
&\|S_{H_R^{d,T}}f - S^{\Lambda(\boldsymbol{z},M)}_{H_R^{d,T}}f|\mathcal{A}(\mathbb{T}^d)\| \\
&\quad\le \Big(\sum_{\boldsymbol{k}\notin H_R^{d,T}}(1+\|\boldsymbol{k}\|_2^2)^{-\beta}\prod_{s=1}^d(1+|k_s|^2)^{-\alpha}\Big)^{\frac12}\Big(\sum_{\boldsymbol{k}\notin H_R^{d,T}}(1+\|\boldsymbol{k}\|_2^2)^{\beta}\prod_{s=1}^d(1+|k_s|^2)^{\alpha}|\hat f_{\boldsymbol{k}}|^2\Big)^{\frac12} \\
&\quad\le \Big(\sum_{\boldsymbol{k}\notin H_R^{d,T}}(1+\|\boldsymbol{k}\|_2^2)^{-\beta}\prod_{s=1}^d(1+|k_s|^2)^{-\alpha}\Big)^{\frac12}\|f|\mathcal{H}^{\alpha,\beta}(\mathbb{T}^d)\|.
\end{aligned}$$

Now we are in the same situation as in (4.7). Therefore we achieve

$$\|S_{H_R^{d,T}}f - S^{\Lambda(\boldsymbol{z},M)}_{H_R^{d,T}}f|\mathcal{A}(\mathbb{T}^d)\| \lesssim \|f|\mathcal{H}^{\alpha,\beta}(\mathbb{T}^d)\|2^{-(\alpha+\beta-\frac12)R}\begin{cases} R^{\frac{d-1}{2}} & :\ \beta=0,\\ 1 & :\ \beta<0.\end{cases}$$

Here, we would like to particularly mention that the aliasing error has the same order as the truncation error. ■

Proposition 4.9. Let the smoothness parameter $\alpha>\frac12$ and $\beta\le 0$ with $\alpha+\beta>\frac12$, the dimension $d\in\mathbb{N}$, $d\ge 2$, and the refinement $R\ge 1$, be given. In addition, we assume that $\Lambda(\boldsymbol{z},M)$ is a reconstructing rank-1 lattice for $H_R^{d,T}$ with $T:=-\frac{\beta}{\alpha}$ constructed by the CBC strategy [14, Tab. 3.1]. We estimate the error of the sampling operator $\mathrm{Id}-S^{\Lambda(\boldsymbol{z},M)}_{H_R^{d,T}}$ by

$$\begin{aligned}
\|\mathrm{Id}-S^{\Lambda(\boldsymbol{z},M)}_{H_R^{d,T}}|\mathcal{H}^{\alpha,\beta}(\mathbb{T}^d)\to L_\infty(\mathbb{T}^d)\| &\lesssim 2^{-(\alpha+\beta-\frac12)R}\begin{cases} R^{\frac{d-1}{2}} & :\ \beta=0,\\ 1 & :\ \beta<0\end{cases}\\
&\lesssim M^{-(\alpha+\beta-\frac12)/2}\begin{cases}(\log M)^{\frac{d-2}{2}(\alpha-\frac12)+\frac{d-1}{2}} & :\ \beta=0,\\ 1 & :\ \beta<0.\end{cases}
\end{aligned}$$

Remark 4.10. In case $\beta<0$ the technique used in the proof of Theorem 4.8 and Proposition 4.9 allows it to benefit from smaller index sets $H_R^{d,T}$ with $T>0$, so called energy-type hyperbolic crosses. Therefore, we obtain no logarithmic dependencies in the error rate.

5 The two-dimensional case

In this chapter we restrict our considerations to two-dimensional approximation problems, i.e., the dimension $d=2$ is fixed. We collect some basic facts from above on this special case.

Lemma 5.1. *Let $R\ge 0$, and $T\in[0,1)$ be given. Each reconstructing rank-1 lattice $\Lambda(\boldsymbol{z},M)$ for the frequency index set $H_R^{2,T}\subset\mathbb{Z}^2$ fulfills*

- $M\ge 2^{2\lfloor R\rfloor}$,
- *$\Lambda(\boldsymbol{z},M)$ is a reconstructing rank-1 lattice for the tensor product grid $G_R^2:=(-2^{\lfloor R\rfloor-1},2^{\lfloor R\rfloor-1}]^2\cap\mathbb{Z}^2$.*

Moreover, there exist reconstructing rank-1 lattices $\Lambda(\boldsymbol{z}, M)$ for the frequency index sets $H_R^{2,T}$ that fulfill $M = (1 + 3 \cdot 2^{\lceil R \rceil - 1}) 2^{\lceil R \rceil} \leq 2^{2R+3}$.

Proof. The proof follows from [17, Theorem 3.5 and Lemma 3.7] and the embeddings $H_R^{2,T} \subset H_R^{2,0}$ for $T \geq 0$, which is direct consequence of the definition. ∎

We interpret the last lemma. The reconstruction property of reconstructing rank-1 lattices $\Lambda(\boldsymbol{z}, M)$ for two-dimensional hyperbolic crosses $H_R^{2,T} \subset (-2^R, 2^R]^2 \cap \mathbb{Z}^2$ implies automatically that the rank-1 lattices $\Lambda(\boldsymbol{z}, M)$ are reconstructing rank-1 lattices for only mildly lower expanded full grids $(-2^{\lfloor R \rfloor - 1}, 2^{\lfloor R \rfloor - 1}]^2 \cap \mathbb{Z}^2$. Accordingly, in the sense of sampling numbers it seems appropriate to use a rank-1 lattice sampling in combination with tensor product grids as frequency index sets in order to even approximate functions of dominating mixed smoothness in dimensions $d = 2$. Thus, we consider the sampling operator $S_{G_R^2}^{\Lambda(\boldsymbol{z},M)}$, cf. (2.3).

Lemma 5.2. *Let $a \in \mathbb{R}$, $0 < a < 1$ and $L \in \mathbb{N}$ be given. Then we estimate*

$$\sum_{\substack{\boldsymbol{j} \in \mathbb{N}_0^2 \\ \|\boldsymbol{j}\|_\infty \geq L}} a^{\|\boldsymbol{j}\|_1} \leq \frac{2 - a^L}{(1-a)^2} a^L \leq C_a \cdot a^L.$$

Proof. We evaluate the geometric series and get

$$\begin{aligned} \sum_{\substack{\boldsymbol{j} \in \mathbb{N}_0^2 \\ \|\boldsymbol{j}\|_\infty \geq L}} a^{\|\boldsymbol{j}\|_1} &= \sum_{j_1=0}^{L-1} a^{j_1} \sum_{j_2=L}^{\infty} a^{j_2} + \sum_{j_2=0}^{L-1} a^{j_2} \sum_{j_1=L}^{\infty} a^{j_1} + \sum_{j_1=L}^{\infty} a^{j_1} \sum_{j_2=L}^{\infty} a^{j_2} \\ &= \left(\frac{1-a^L}{1-a} + \frac{1-a^L}{1-a} + \frac{a^L}{1-a} \right) \frac{a^L}{1-a}. \end{aligned}$$

∎

Theorem 5.3. *Let the smoothness parameter $\alpha > \frac{1}{2}, \gamma \geq 0$ with $\alpha > \gamma$ and the refinement $R \geq 0$, be given. In addition, we assume that $\Lambda(\boldsymbol{z}, M)$ is a reconstructing rank-1 lattice for G_R^2 with $M \asymp 2^{2R}$. We estimate the error of the sampling operator $\mathrm{Id} - S_{G_R^2}^{\Lambda(\boldsymbol{z},M)}$ by*

$$\|\mathrm{Id} - S_{G_R^2}^{\Lambda(\boldsymbol{z},M)} | \mathcal{H}_{\mathrm{mix}}^\alpha(\mathbb{T}^2) \to \mathcal{H}^\gamma(\mathbb{T}^2)\| \asymp M^{-(\alpha-\gamma)/2}.$$

Proof. The lower bound goes back to Theorem 3.2. The proof of the upper bound is similar to the proof of Theorem 4.4. The main difference is that we use the full grid G_R^2 instead of $H_R^{2,0}$ here. This yields for the projection

$$\|\mathrm{Id} - S_{G_R^2} | \mathcal{H}_{\mathrm{mix}}^\alpha(\mathbb{T}^2) \to \mathcal{H}^\gamma(\mathbb{T}^2)\| \lesssim M^{-(\alpha-\gamma)/2}.$$

The estimation for the aliasing error $\|S_{G_R^2} f - S_{G_R^2}^{\Lambda(\boldsymbol{z},M)} f | \mathcal{H}^\gamma(\mathbb{T}^2)\|$ is also very similar to (4.4). We follow the proof line by line with the mentioned modification and come to the estimation

$$\begin{aligned} &\|S_{G_R^2} f - S_{G_R^2}^{\Lambda(\boldsymbol{z},M)} f | \mathcal{H}^\gamma(\mathbb{T}^2)\| \\ &\quad \leq \sup_{\boldsymbol{k} \in G_R^2} \Big((1 + \|\boldsymbol{k}\|_2^2)^\gamma \sum_{\boldsymbol{j} \in \mathbb{N}_0^d} \sum_{\substack{\boldsymbol{h} \in \Lambda(\boldsymbol{z},M)^\perp \\ \boldsymbol{h} \neq \boldsymbol{0}}} \varphi_{\boldsymbol{j}}(\boldsymbol{k} + \boldsymbol{h}) \prod_{i=1}^d (1 + |k_i + h_i|^2)^{-\alpha} \Big)^{\frac{1}{2}} \|f | \mathcal{H}_{\mathrm{mix}}^\alpha(\mathbb{T}^2)\|. \end{aligned}$$

Due to the reproduction property for G_R^2 the sum over $\boldsymbol{j}$ breaks down to

$$\begin{aligned}\|S_{G_R^2} f - S_{G_R^2}^{\Lambda(\boldsymbol{z},M)} f|\mathcal{H}^\gamma(\mathbb{T}^2)\| \\ \lesssim \sup_{\boldsymbol{k}\in G_R^2} \Big((1+\|\boldsymbol{k}\|_2^2)^\gamma \sum_{\|\boldsymbol{j}\|_\infty > \lfloor R\rfloor} 2^{-2\alpha\|\boldsymbol{j}\|_1} \sum_{\substack{\boldsymbol{h}\in\Lambda(\boldsymbol{z},M)^\perp \\ \boldsymbol{h}\neq\boldsymbol{0}}} \varphi_{\boldsymbol{j}}(\boldsymbol{k}+\boldsymbol{h})\Big)^{\frac{1}{2}} \|f|\mathcal{H}_{\mathrm{mix}}^\alpha(\mathbb{T}^2)\|.\end{aligned}$$

Next, we recognize

$$\sup_{\boldsymbol{k}\in G_R^2} (1+\|\boldsymbol{k}\|_2^2)^{\frac{\gamma}{2}} \lesssim 2^{\gamma R}. \tag{5.1}$$

Using $H_{R-2}^{d,0} \subset G_R^2$, we obtain $\Lambda(\boldsymbol{z},M)^\perp \cap H_{R-2}^{d,0} = \{\boldsymbol{0}\}$. We apply Lemma 4.1 and employ $R-1 \leq \lfloor R\rfloor \leq \|\boldsymbol{j}\|_\infty \leq \|\boldsymbol{j}\|_1$ to see

$$\begin{aligned}\|S_{G_R^2} f - S_{G_R^2}^{\Lambda(\boldsymbol{z},M)} f|\mathcal{H}^\gamma(\mathbb{T}^2)\| \\ \lesssim 2^{\gamma R}\Big(2^{-R} \sum_{\|\boldsymbol{j}\|_\infty > \lfloor R\rfloor} 2^{-(2\alpha-1)\|\boldsymbol{j}\|_1}\Big)^{\frac{1}{2}} \|f|\mathcal{H}_{\mathrm{mix}}^\alpha(\mathbb{T}^2)\|.\end{aligned}$$

Applying Lemma 5.2 yields

$$\begin{aligned}\|S_{G_R^2} f - S_{G_R^2}^{\Lambda(\boldsymbol{z},M)} f|\mathcal{H}^\gamma(\mathbb{T}^2)\| &\lesssim 2^{-(\alpha-\gamma)R}\|f|\mathcal{H}_{\mathrm{mix}}^\alpha(\mathbb{T}^2)\| \\ &\lesssim M^{-(\alpha-\gamma)/2}\|f|\mathcal{H}_{\mathrm{mix}}^\alpha(\mathbb{T}^2)\|.\end{aligned}$$

■

Remark 5.4. This method does not work for $\mathcal{H}_{\mathrm{mix}}^\gamma(\mathbb{T}^2)$ as target space. Here the estimation of the mixed weight, similar to (5.1) implies a worse main rate for the asymptotic behavior of $\|S_{G_R^2} f - S_{G_R^2}^{\Lambda(\boldsymbol{z},M)} f|\mathcal{H}_{\mathrm{mix}}^\gamma(\mathbb{T}^2)\|$. Here we have to use $H_R^{2,0}$ as index set for our trigonometric polynomials and therefore Theorem 4.4 is the best we have in this situation.

Theorem 5.5. *Let the smoothness parameter $\alpha > \frac{1}{2}$ and the refinement $R \geq 0$ be given. In addition, we assume that $\Lambda(\boldsymbol{z},M)$ is a reconstructing rank-1 lattice for G_R^2 with $M \asymp 2^{2R}$. We estimate the error of the sampling operator* $\mathrm{Id} - S_{G_R^2}^{\Lambda(\boldsymbol{z},M)}$ *by*

$$\|\mathrm{Id} - S_{G_R^2}^{\Lambda(\boldsymbol{z},M)}|\mathcal{H}_{\mathrm{mix}}^\alpha(\mathbb{T}^2) \to \mathcal{A}(\mathbb{T}^2)\| \lesssim M^{-(\alpha-\frac{1}{2})/2}.$$

Proof. The result is a consequence of replacing $H_R^{2,0}$ by G_R^2 in the proof of Theorem 4.8. ■

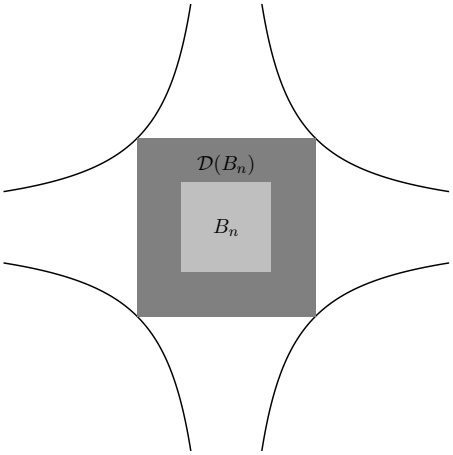

Figure 5.1: Relations between $B_n, \mathcal{D}(B_n)$ and a hyperbolic cross of size δb_n.

Proposition 5.6. Let the smoothness parameter $\alpha > \frac{1}{2}$ and the refinement $R \geq 0$, be given. In addition, we assume that $\Lambda(\boldsymbol{z}, M)$ is a reconstructing rank-1 lattice for G_R^2 with $M \asymp 2^{2R}$. We estimate the error of the sampling operator $\mathrm{Id} - S_{G_R^2}^{\Lambda(\boldsymbol{z},M)}$ by

$$\|\mathrm{Id} - S_{G_R^2}^{\Lambda(\boldsymbol{z},M)} | \mathcal{H}_{\mathrm{mix}}^{\alpha}(\mathbb{T}^2) \to L_\infty(\mathbb{T}^2)\| \lesssim M^{-(\alpha-\frac{1}{2})/2}. \qquad \blacksquare$$

Now we come to the second very special property of the 2-dimensional situation. Here we know closed formulas for lattices that are reconstructing for $H_R^{2,0}$ (and G_R^2). The well studied Fibonacci lattice $F_n = \Lambda(\boldsymbol{z}, b_n)$, where $\boldsymbol{z} = (1, b_{n-1})$ and $M = b_n$ gives a universal reconstructing rank-1 lattice for index sets considered in this chapter. The Fibonacci numbers b_n are defined iteratively by

$$b_0 = b_1 = 1, \quad b_n = b_{n-1} + b_{n-2},\ n \geq 2.$$

Since the size of the Fibonacci lattice depends on $M = b_n$, we go the other way around. For a fixed refinement $n \in \mathbb{N}$ we choose a suitable rectangle B_n for which the reproduction property (2.7) is fulfilled. Let us start with the box

$$B_n := \left[-\left\lfloor C\sqrt{b_n} \right\rfloor, \left\lfloor C\sqrt{b_n} \right\rfloor \right]^2 \cap \mathbb{Z}^2,$$

where $C > 0$ is a suitable constant. Obviously, the difference set of such a box fulfills

$$\mathcal{D}(B_n) = \left[-2\left\lfloor C\sqrt{b_n} \right\rfloor, 2\left\lfloor C\sqrt{b_n} \right\rfloor \right]^2 \cap \mathbb{Z}^2.$$

It is known (see Lemma IV.2.1 in [39]), that there is a $\delta > 0$ such that for all frequencies of the dual lattice $F_n^\perp$ of F_n

$$\prod_{s=1}^{2} \max\{1, |h_s|\} \geq \delta b_n$$

holds. For that reason we find a $C > 0$ (depending only on δ) such that the property

$$\mathcal{D}(B_n) \cap F_n^\perp = \{0\}$$

is fulfilled for all $n \in \mathbb{N}$ (see Figure 5.1), which guarantees the reproduction property for the index set B_n. Additionally we have $|B_n| \asymp b_n$. Therefore, the Fibonacci lattice fulfills the properties mentioned in Lemma 5.1.

6 Further comments

6.1 Minkowski's theorem in Section 3

Remark 6.1. In order to show the lower bounds in Theorem 3.2, one may alternatively use Minkowski's theorem instead of the construction in Lemma 3.1. Then the main rate in M is identical but one obtains an additional factor that decreases exponentially in the dimension d in the lower bound.

6.2 Hyperbolic cross property in Section 4

The following remark is hypothetical since it is an open question whether a lattice with the so-called "hyperbolic cross property" exists in $d > 2$, cf. Lemma 2.3.

Remark 6.2. Let $\Lambda(\boldsymbol{z}, M)$ be a lattice such that $\Lambda(\boldsymbol{z}, M)^\perp \cap H_{2R}^{d,0} = \{0\}$ with $M \asymp 2^{2R}$ holds. We call this property "hyperbolic cross property". Then

$$\begin{aligned}\|f - S_{H_R^{d,0}}^{\Lambda(\boldsymbol{z},M)} f | \mathcal{H}^\gamma(\mathbb{T}^d)\| &\lesssim 2^{-(\alpha-\gamma)R} R^{\frac{d-1}{2}} \|f|\mathcal{H}^\alpha_{\mathrm{mix}}(\mathbb{T}^d)\| \\ &\asymp M^{-\frac{\alpha-\gamma}{2}} (\log M)^{\frac{d-1}{2}}.\end{aligned}$$

Proof. Computing the truncation error is straight-forward. For the aliasing error we get

$$\begin{aligned}&\|S_{H_R^{d,0}} f - S_{H_R^{d,0}}^{\Lambda(\boldsymbol{z},M)} f|\mathcal{H}^\gamma(\mathbb{T}^d)\| \\ &\leq \sup_{\boldsymbol{k}\in H_R^{d,0}} \Big((1+\|\boldsymbol{k}\|_2^2)^\gamma \sum_{\boldsymbol{j}\notin J_R^{d,0}} \sum_{\substack{\boldsymbol{h}\in\Lambda(\boldsymbol{z},M)^\perp \\ \boldsymbol{h}\neq\boldsymbol{0}}} \varphi_{\boldsymbol{j}}(\boldsymbol{k}+\boldsymbol{h}) \prod_{s=1}^d (1+|k_s+h_s|^2)^{-\alpha}\Big)^{\frac{1}{2}} \|f|\mathcal{H}^\alpha_{\mathrm{mix}}(\mathbb{T}^d)\|.\end{aligned}$$

Now we use the fact that the difference set $\mathcal{D}(H_R^{d,0})$ is contained in $H_{c+2R}^{d,0}$ and therefore, $\Lambda(\boldsymbol{z}, M)$ is reproducing for $H_R^{d,0}$ (the dual lattice is located outside of the difference set). With the usual calculation we get then

$$\begin{aligned}&\|S_{H_R^{d,0}} f - S_{H_R^{d,0}}^{\Lambda(\boldsymbol{z},M)} f|\mathcal{H}^\gamma(\mathbb{T}^d)\| \\ &\lesssim \sup_{\boldsymbol{k}\in H_R^{d,0}} (1+\|\boldsymbol{k}\|_2^2)^{\frac{\gamma}{2}} \Big(\sum_{R<\|\boldsymbol{j}\|_1<2R} 2^{-2\alpha\|\boldsymbol{j}\|_1} + \sum_{\|\boldsymbol{j}\|_1>2R} 2^{-2\alpha\|\boldsymbol{j}\|_1} \frac{2^{\|\boldsymbol{j}\|_1}}{2^{2R}}\Big)^{\frac{1}{2}} \\ &\lesssim 2^{-(\alpha-\gamma)R} R^{\frac{d-1}{2}} \|f|\mathcal{H}^\alpha_{\mathrm{mix}}(\mathbb{T}^d)\| \\ &\asymp M^{-\frac{\alpha-\gamma}{2}} (\log M)^{\frac{d-1}{2}} \|f|\mathcal{H}^\alpha_{\mathrm{mix}}(\mathbb{T}^d)\|.\end{aligned}$$

■

Unfortunately, if $d > 2$ such a lattice is not known. We see that even in this "ideal" case we do not get rid of the $(\log M)^{\frac{d-1}{2}}$. If $d = 2$ we get rid of both logs, see Section 5. One reason is that e.g. the Fibonacci lattice has a "hyperbolic cross property" (cf. Remark 6.2). The other reason is that due to the "half rate" we can truncate from a larger set than the hyperbolic cross. In that sense $d = 2$ is a very specific case.

6.3 Energy-norm setting in Section 4

Remark 6.3. Additionally to the considerations in Proposition 4.6 it seems natural to treat the cases $\gamma > \beta > 0$. One would expect from the theory of sparse grids that a modification of the hyperbolic cross index sets $H_R^{d,0}$ to energy-norm based hyperbolic crosses $H_R^{d,T}$ with $T = \frac{\gamma-\beta}{\alpha}$ or a little perturbation of it would help to reduce logarithmic dependence on M. Unfortunately, we are currently not able to improve or even get equivalent results for that. One reason is that we have no improved results fitting $H_R^{d,T}$ in Lemma 4.1. The other reason is that in case $\gamma > 0$ we have not yet found a way to exploit smoothness that come from the target space such that one can use smaller index sets than $H_R^{d,0}$ in the error sum. Our standard estimation yields a worse main rate for that.

6.4 Sampling along multiple rank-1 lattices

Similar to sampling along sparse grids, which are unions of anisotropic full grids, one may use the union of several rank-1 lattices as sampling set, cf. [16]. In contrast to the CBC approach of reconstructing rank-1 lattices, that uses a single rank-1 lattice as sampling scheme, one builds up finite sequences of rank-1 lattices which allow for the exact reconstruction of trigonometric polynomials. Numerical tests suggest significantly lower numbers M of sampling nodes that are required. In detail, numerical tests in [16] seem to promise constant oversampling factors $M/|H_R^{d,0}|$. Accordingly, the sampling rates could be possibly similar to those of sparse grids.

7 Results for anisotropic mixed smoothness

In this section we give an outlook on function spaces $\mathcal{H}^{\boldsymbol{\alpha}}_{\mathrm{mix}}(\mathbb{T})$ where $\boldsymbol{\alpha}$ is a vector with first μ smallest smoothness directions, i.e.,

$$\frac{1}{2} < \alpha_1 = \ldots = \alpha_\mu < \alpha_{\mu+1} \leq \ldots \leq \alpha_d.$$

Definition 7.1. *Let $\boldsymbol{\alpha} \in \mathbb{R}^d$ with positive entries. We define the Sobolev spaces with anisotropic mixed smoothness $\boldsymbol{\alpha}$ as*

$$\mathcal{H}^{\boldsymbol{\alpha}}_{\mathrm{mix}}(\mathbb{T}^d) := \left\{ f \in L_2(\mathbb{T}^d) \colon \|f|\mathcal{H}^{\boldsymbol{\alpha}}_{\mathrm{mix}}(\mathbb{T}^d)\|^2 := \sum_{\boldsymbol{k}\in\mathbb{Z}^d} |\hat{f}_{\boldsymbol{k}}|^2 \prod_{s=1}^{d} (1+|k_s|^2)^{\alpha_s} < \infty \right\}.$$

Again, we want to study approximation by sampling along rank-1 lattices. Therefore we introduce new index sets, so-called anisotropic hyperbolic crosses $H_R^{d,\boldsymbol{\alpha}}$ defined by

$$H_R^{d,\boldsymbol{\alpha}} := \bigcup_{\boldsymbol{j}\in J_R^{d,\boldsymbol{\alpha}}} Q_{\boldsymbol{j}}$$

where

$$J_R^{d,\boldsymbol{\alpha}} := \Big\{ \boldsymbol{j} \in \mathbb{N}_0^d \colon \frac{1}{\alpha_1} \boldsymbol{\alpha} \cdot \boldsymbol{j} \leq R \Big\}.$$

Lemma 7.2. *Let $\boldsymbol{\alpha} \in \mathbb{R}^d$ with $0 < \alpha_1 = \ldots = \alpha_\mu < \alpha_{\mu+1} \leq \ldots \leq \alpha_d$. Then*

$$|H_R^{d,\boldsymbol{\alpha}}| \asymp \sum_{\boldsymbol{j} \in J_R^{d,\boldsymbol{\alpha}}} 2^{\|\boldsymbol{j}\|_1} \asymp 2^R R^{\mu-1}.$$

Proof. For the upper bound we refer to [38, Chapt. 1., Lem. D]. For the lower bound we consider the subset

$$J_{R,\mu}^{d,\boldsymbol{\alpha}} := \{ \boldsymbol{j} \in J_R^{d,\boldsymbol{\alpha}} : j_{\mu+1} = \ldots = j_d = 0 \} \subset J_R^{d,\boldsymbol{\alpha}}$$

and obtain with the help of Lemma 2.2

$$\sum_{\boldsymbol{j} \in J_R^{d,\boldsymbol{\alpha}}} 2^{\|\boldsymbol{j}\|_1} \geq \sum_{\boldsymbol{j} \in J_{R,\mu}^{d,\boldsymbol{\alpha}}} 2^{\|\boldsymbol{j}\|_1} \asymp \sum_{\boldsymbol{j} \in J_{R+c}^{\mu,0}} 2^{\|\boldsymbol{j}\|_1} \gtrsim 2^R R^{\mu-1}.$$

■

Lemma 7.3. *Let the refinement $R \geq 1$, and the dimension $d \in \mathbb{N}$ with $d \geq 2$, be given. Then there exists a reconstructing rank-1 lattice $\Lambda(\boldsymbol{z}, M)$ for $H_R^{d,\boldsymbol{\alpha}}$ which fulfills*

$$2^R R^{\mu-1} \asymp |H_R^{d,\boldsymbol{\alpha}}| \leq M \lesssim 2^{2R} R^{\mu-1}.$$

Proof. First, we show the embedding of the difference set $\mathcal{D}(H_R^{d,\boldsymbol{\alpha}}) \subset H_{2R+\|\boldsymbol{\alpha}\|_1}^{d,\boldsymbol{\alpha}}$. Let $\boldsymbol{k}, \boldsymbol{k'} \in H_R^{d,\boldsymbol{\alpha}}$. Then there exist indices $\boldsymbol{j}, \boldsymbol{j'} \in J_R^{d,\boldsymbol{\alpha}}$ such that $\boldsymbol{k} \in Q_{\boldsymbol{j}}$ and $\boldsymbol{k'} \in Q_{\boldsymbol{j'}}$. The difference $\boldsymbol{k} - \boldsymbol{k'} \in \mathcal{D}(H_R^{d,\boldsymbol{\alpha}})$ and $\boldsymbol{k} - \boldsymbol{k'} \in Q_{\tilde{\boldsymbol{j}}}$ for an index $\tilde{\boldsymbol{j}} \in \mathbb{N}_0^d$. Next, we show $\boldsymbol{\alpha} \cdot \tilde{\boldsymbol{j}} \leq 2R + \|\boldsymbol{\alpha}\|_1$. The differences $k_s - k_s'$ of one component of $\boldsymbol{k}$ and $\boldsymbol{k'}$ fulfill

$$k_s - k_s' \in [-2^{j_s} - 2^{j_s'}, 2^{j_s} + 2^{j_s'}] \subset [-2^{\max(j_s, j_s')+1}, 2^{\max(j_s, j_s')+1}] = \bigcup_{t=0}^{\max(j_s, j_s')+1} Q_t$$

and we obtain $\tilde{j}_s \leq \max(j_s, j_s') + 1 \leq j_s + j_s' + 1$. This yields $\boldsymbol{\alpha} \cdot \tilde{\boldsymbol{j}} \leq \boldsymbol{\alpha} \cdot \boldsymbol{j} + \boldsymbol{\alpha} \cdot \boldsymbol{j'} + \|\boldsymbol{\alpha}\|_1 \leq 2R + \|\boldsymbol{\alpha}\|_1$ and consequently the embedding $\mathcal{D}(H_R^{d,\boldsymbol{\alpha}}) \subset H_{2R+\|\boldsymbol{\alpha}\|_1}^{d,\boldsymbol{\alpha}}$ holds. Finally, the assertion is a consequence of Lemma 7.2 and [14, Corollary 3.4]. ■

Remark 7.4. The proof of Lemma 7.3 referred here is based on an abstract result suitable for much more general index sets than $H_R^{d,\boldsymbol{\alpha}}$. Similar to Lemma 2.3 there should be also a direct computation for counting the cardinality of the difference set $\mathcal{D}(H_R^{d,\boldsymbol{\alpha}})$. We leave the details to the interested reader.

Lemma 7.5. *Let $\boldsymbol{\alpha}, \boldsymbol{\gamma} \in \mathbb{R}^d$ with $\frac{1}{2} < \alpha_1 = \gamma_1 = \ldots = \alpha_\mu = \gamma_\mu < \alpha_{\mu+1} \leq \ldots \leq \alpha_d$ with $\alpha_\mu < \gamma_s < \alpha_s$ for $s = \mu+1, \ldots, d$. Then it holds*

$$\sum_{\boldsymbol{j} \in \mathbb{N}_0^d \setminus J_R^{d,\boldsymbol{\gamma}}} 2^{-(2\boldsymbol{\alpha}-\mathbf{1})\cdot \boldsymbol{j}} \lesssim 2^{-(2\alpha_1-1)R} R^{\mu-1}.$$

Proof. We start decomposing the sum. For technical reasons we introduce the notation

$$P_R^{d,\boldsymbol{\gamma}} := \Big\{ \boldsymbol{j} \in \mathbb{N}_0^d : \frac{\gamma_s}{\gamma_1} j_s \leq R, s = 1, \ldots, d \Big\}.$$

Since $J_R^{d,\boldsymbol{\gamma}} \subset P_R^{d,\boldsymbol{\gamma}}$ we obtain

$$\sum_{\boldsymbol{j} \in \mathbb{N}_0^d \setminus J_R^{d,\boldsymbol{\gamma}}} 2^{-(2\boldsymbol{\alpha}-\mathbf{1})\cdot \boldsymbol{j}} = \sum_{\substack{\boldsymbol{j} \notin J_R^{d,\boldsymbol{\gamma}} \\ \boldsymbol{j} \in P_R^{d,\boldsymbol{\gamma}}}} 2^{-(2\boldsymbol{\alpha}-\mathbf{1})\cdot \boldsymbol{j}} + \sum_{\boldsymbol{j} \in \mathbb{N}_0^d \setminus P_R^{d,\boldsymbol{\gamma}}} 2^{-(2\boldsymbol{\alpha}-\mathbf{1})\cdot \boldsymbol{j}}. \tag{7.1}$$

We estimate the first summand in (7.1)

$$\begin{aligned}
\sum_{\substack{\boldsymbol{j} \notin J_R^{d,\boldsymbol{\gamma}} \\ \boldsymbol{j} \in P_R^{d,\boldsymbol{\gamma}}}} 2^{-(2\boldsymbol{\alpha}-\mathbf{1})\cdot \boldsymbol{j}} &= \sum_{j_d=0}^{\frac{\gamma_1 R}{\gamma_d}} 2^{-(2\alpha_d-1)j_d} \cdot \ldots \cdot \sum_{j_{\mu+1}=0}^{\frac{\gamma_1 R}{\gamma_{\mu+1}}} 2^{-(2\alpha_{\mu+1}-1)j_{\mu+1}} \\
&\quad \cdot \sum_{j_\mu=0}^{\frac{\gamma_1 R}{\gamma_\mu}} 2^{-(2\alpha_\mu-1)j_\mu} \cdot \ldots \cdot \sum_{j_2=0}^{\frac{\gamma_1 R}{\gamma_2}} 2^{-(2\alpha_2-1)j_2} \sum_{j_1=\frac{\gamma_1 R - \sum_{s=2}^d \gamma_s j_s}{\gamma_1}}^{R} 2^{-(2\alpha_1-1)j_2} \\
&\lesssim \sum_{j_d=0}^{\frac{\gamma_1 R}{\gamma_d}} 2^{-(2\alpha_d-1)j_d} \cdot \ldots \cdot \sum_{j_{\mu+1}=0}^{\frac{\gamma_1 R}{\gamma_{\mu+1}}} 2^{-(2\alpha_{\mu+1}-1)j_{\mu+1}} \\
&\quad \cdot \sum_{j_\mu=0}^{\frac{\gamma_1 R}{\gamma_\mu}} 2^{-(2\alpha_\mu-1)j_\mu} \cdot \ldots \cdot \sum_{j_2=0}^{\frac{\gamma_1 R}{\gamma_2}} 2^{-(2\alpha_2-1)j_2} 2^{-(2\alpha_1-1)\frac{\gamma_1 R - \sum_{s=2}^d \gamma_s j_s}{\gamma_1}}.
\end{aligned}$$

Interchanging the order of multiplication yields

$$\begin{aligned}
\sum_{\substack{\boldsymbol{j} \notin J_R^{d,\boldsymbol{\gamma}} \\ \boldsymbol{j} \in P_R^{d,\boldsymbol{\gamma}}}} 2^{-(2\boldsymbol{\alpha}-\mathbf{1})\cdot \boldsymbol{j}} &\lesssim 2^{-(2\alpha_1-1)R} \sum_{j_d=0}^{\infty} 2^{-[(2\alpha_d-1)-(2\gamma_d-\frac{\gamma_d}{\alpha_1})]j_d} \cdot \ldots \\
&\quad \cdot \sum_{j_{\mu+1}=0}^{\infty} 2^{-[(2\alpha_{\mu+1}-1)-(2\gamma_{\mu+1}-\frac{\gamma_{\mu+1}}{\alpha_1})]j_{\mu+1}} \cdot \sum_{j_\mu=0}^{\frac{R}{\gamma_\mu-\varepsilon}} 1 \cdot \ldots \cdot \sum_{j_2=0}^{\frac{R}{\gamma_2-\varepsilon}} 1 \\
&\lesssim 2^{-(2\alpha_1-1)R} R^{\mu-1}.
\end{aligned}$$

The second summand in (7.1) can be trivially estimated by $\lesssim 2^{-(2\alpha_1-1)R}$. ∎

Theorem 7.6. *Let* $\boldsymbol{\alpha}, \boldsymbol{\gamma} \in \mathbb{R}^d$ *such that*

$$\frac{1}{2} < \alpha_1 = \gamma_1 = \ldots = \alpha_\mu = \gamma_\mu < \alpha_{\mu+1} \leq \ldots \leq \alpha_d$$

and

$$\alpha_1 < \gamma_s < \alpha_s, \ s = \mu+1, \ldots, d,$$

and the refinement $R \geq 1$*, be given. In addition, we assume that* $\Lambda(\boldsymbol{z}, M)$ *is a reconstructing rank-1 lattice for* $H_R^{d,\boldsymbol{\gamma}}$ *constructed by the CBC strategy [14, Tab. 3.1]. We estimate the error of the sampling operator* $\mathrm{Id} - S_{H_R^{d,\boldsymbol{\gamma}}}^{\Lambda(\boldsymbol{z},M)}$ *by*

$$\begin{aligned}\|\mathrm{Id} - S_{H_R^{d,\boldsymbol{\gamma}}}^{\Lambda(\boldsymbol{z},M)} | \mathcal{H}_{\mathrm{mix}}^{\boldsymbol{\alpha}}(\mathbb{T}^d) \to L_\infty(\mathbb{T}^d)\| &\lesssim 2^{-(\alpha_1 - \frac{1}{2})R} R^{\frac{\mu-1}{2}} \\ &\lesssim M^{-(\alpha_1-\frac{1}{2})/2} (\log M)^{\frac{\mu-1}{2}(\alpha_1+\frac{1}{2})}.\end{aligned}$$

Proof. We use the embedding $\mathcal{A}(\mathbb{T}^d) \hookrightarrow L_\infty(\mathbb{T}^d)$ and follow the estimation of Theorem 4.8 where we replace the weight $\prod_{s=1}^d (1+|k_s|^2)^\alpha$ by $\prod_{s=1}^d (1+|k_s|^2)^{\alpha_s}$. We obtain

$$\|f - S_{H_R^{d,\boldsymbol{\gamma}}}^{\Lambda(\boldsymbol{z},M)} f | L_\infty(\mathbb{T}^d)\| \lesssim \left(\sum_{\boldsymbol{j} \in \mathbb{N}_0^d \setminus J_R^{d,\boldsymbol{\gamma}}} 2^{-(2\boldsymbol{\alpha}-\mathbf{1})\cdot \boldsymbol{j}} \right)^{\frac{1}{2}} \|f | \mathcal{H}_{\mathrm{mix}}^{\boldsymbol{\alpha}}(\mathbb{T}^d)\|.$$

Applying Lemma 7.5 yields

$$\|f - S_{H_R^{d,\boldsymbol{\gamma}}}^{\Lambda(\boldsymbol{z},M)} f | L_\infty(\mathbb{T}^d)\| \lesssim 2^{-(\alpha_1-\frac{1}{2})R} R^{\frac{\mu-1}{2}} \|f | \mathcal{H}_{\mathrm{mix}}^{\boldsymbol{\alpha}}(\mathbb{T}^d)\|.$$

Now the bound for the number of points in Lemma 7.3 implies

$$\|f - S_{H_R^{d,\boldsymbol{\gamma}}}^{\Lambda(\boldsymbol{z},M)} f | L_\infty(\mathbb{T}^d)\| \lesssim M^{-(\alpha_1-\frac{1}{2})/2} (\log M)^{\frac{\mu-1}{2}(\alpha_1+\frac{1}{2})} \|f | \mathcal{H}_{\mathrm{mix}}^{\boldsymbol{\alpha}}(\mathbb{T}^d)\|.$$

That proves the claim. ∎

Remark 7.7. Comparing the last result with the results obtained in Proposition 4.9 we recognize that there is only the exponent $\mu - 1$ instead of $d - 1$ in the logarithm of the error term with $\mu < d$. Especially in the case $\mu = 1$ the logarithm completely vanishes. Similar effects were also observed for sparse grids and general linear approximation, cf. [9, 38].

8 Numerical results

In this section, we numerically investigate the sampling rates for different types of rank-1 lattices $\Lambda(\boldsymbol{z}, M)$ when sampling the scaled periodized (tensor product) kink function

$$g(\boldsymbol{x}) := \prod_{t=1}^d \left(\frac{5^{3/4}15}{4\sqrt{3}} \max\left\{ \frac{1}{5} - \left(x_t - \frac{1}{2}\right)^2, 0 \right\} \right), \quad \boldsymbol{x} := (x_1, \ldots, x_d)^\top \in \mathbb{T}^d, \tag{8.1}$$

similar to [12]. We remark that $g \in \mathcal{H}_{\mathrm{mix}}^{3/2-\varepsilon}(\mathbb{T}^d)$, $\varepsilon > 0$, and $\|g | L_2(\mathbb{T}^d)\| = 1$.

For the fast approximate reconstruction, Algorithm 8.1 can be used. This algorithm applies a single one-dimensional fast Fourier transform (FFT) on the function samples and performs a simple index transform. As input parameter a reconstructing rank-1 lattice $\Lambda(\boldsymbol{z}, M)$ is required, which may be easily searched for by means of the CBC strategy [14, Tab. 3.1].

Algorithm 8.1 Fast approximate reconstruction of a function $f \in \mathcal{H}^{\alpha,\beta}(\mathbb{T}^d)$ from sampling values on a reconstructing rank-1 lattice $\Lambda(\boldsymbol{z}, M)$ using a single one-dimensional FFT, see [18, Algorithm 1].

Input:	$I \subset \mathbb{Z}^d$	frequency index set of finite cardinality
	$\Lambda(\boldsymbol{z}, M)$	reconstructing rank-1 lattice for I of size M with generating vector $\boldsymbol{z} \in \mathbb{Z}^d$
	$\boldsymbol{f} = \left(f\left(\frac{j\boldsymbol{z}}{M} \bmod \mathbf{1}\right)\right)_{j=0}^{M-1}$	samples of $f \in \mathcal{H}^{\alpha,\beta}(\mathbb{T}^d)$ on $\Lambda(\boldsymbol{z}, M)$
$\hat{\boldsymbol{a}} := \mathrm{FFT\_1D}(\boldsymbol{f})$		
for each $\boldsymbol{k} \in I$ ***do***		
$\hat{f}_{\boldsymbol{k}}^{\Lambda(\boldsymbol{z},M)} := \frac{1}{M}\, \hat{a}_{\boldsymbol{k}\cdot\boldsymbol{z} \bmod M}$		
end for		
Output:	$\hat{f}_{\boldsymbol{k}}^{\Lambda(\boldsymbol{z},M)}$	Fourier coefficients of the approximation $S_I^{\Lambda(\boldsymbol{z},M)} f$ as defined in (2.3)
Complexity:	$\mathcal{O}\left(M \log M + d\lvert I\rvert\right)$	

8.1 Hyperbolic cross index sets

First, we build reconstructing rank-1 lattices for the hyperbolic cross index sets $H_R^{d,0}$ in the cases $d = 2, 3, 4$ with various refinements $R \in \mathbb{N}_0$ using the CBC strategy [14, Tab. 3.1]. Then, we apply the sampling operators $S_{H_R^{d,0}}^{\Lambda(\boldsymbol{z},M)}$ on the kink function g using Algorithm 8.1. The resulting sampling errors $\|g - S_{H_R^{d,0}}^{\Lambda(\boldsymbol{z},M)} g | L_2(\mathbb{T}^d)\|$ are shown in Figure 8.1 and 8.2 denoted by "CBC hc". The corresponding theoretical upper bounds for the sampling rates from Table 1.2, which are (almost) $M^{-\frac{1}{2}\cdot\frac{3}{2}} (\log M)^{\frac{d-2}{2}\cdot\frac{3}{2}+\frac{d-1}{2}}$, are also depicted. Additionally in the two-dimensional case, we consider the Fibonacci lattices from Section 5 as well as special Korobov lattices

$$\Lambda((1, \lceil 3 \cdot 2^{R-2} \rceil)^\top, \lceil (1 + 3 \cdot 2^{R-2}) \cdot 2^{R-1} \rceil)$$

from [17]. The corresponding sampling errors are denoted by "Fibonacci hc" and "Korobov hc" in Figure 8.1. We observe that in all considered cases, the sampling errors decay approximately as fast as the theoretical upper bound implies. In Figure 8.3, we investigate the logarithmic factors in more detail. Assuming that the sampling error $\|g - S_{H_R^{d,0}}^{\Lambda(\boldsymbol{z},M)} g | L_2(\mathbb{T}^d)\|$ nearly decays like $M^{-\frac{1}{2}\cdot\frac{3}{2}} (\log M)^{\frac{d-2}{2}\cdot\frac{3}{2}+\frac{d-1}{2}}$, we consider its scaled version

$$\|g - S_{H_R^{d,0}}^{\Lambda(\boldsymbol{z},M)} g | L_2(\mathbb{T}^d)\| / [M^{-\frac{1}{2}\cdot\frac{3}{2}} (\log M)^{\frac{d-2}{2}\cdot\frac{3}{2}+\frac{d-1}{2}}].$$

Obviously, if the scaled error decays exactly like the given rate, then the plot should be (approximately) a horizontal line. In the plot in Figure 8.3a for the two-dimensional case, this is almost the case for all three types of lattices. The scaled errors $\|g - S_{H_R^{d,0}}^{\Lambda(\boldsymbol{z},M)} g | L_2(\mathbb{T}^d)\| \cdot M^{1.5/2} \cdot (\log M)^{-1/2}$ seem to decay slightly but the errors in Figure 8.3b, that are scaled without the logarithmic factor, grow slightly. We interpret this observation as an indication that there is some logarithmic dependence in the error rate. Moreover, for the reconstructing rank-1 lattices built using the CBC strategy [14, Tab. 3.1], the scaled errors in the cases $d = 3$, $d = 4$, and $d = 5$ behave similarly as in the two-dimensional case, see Figure 8.3c.

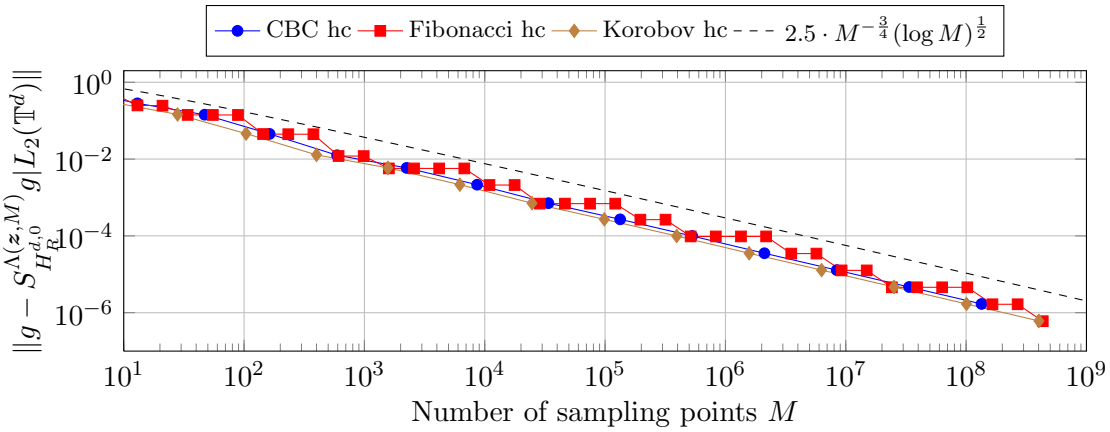

(a) $d = 2$

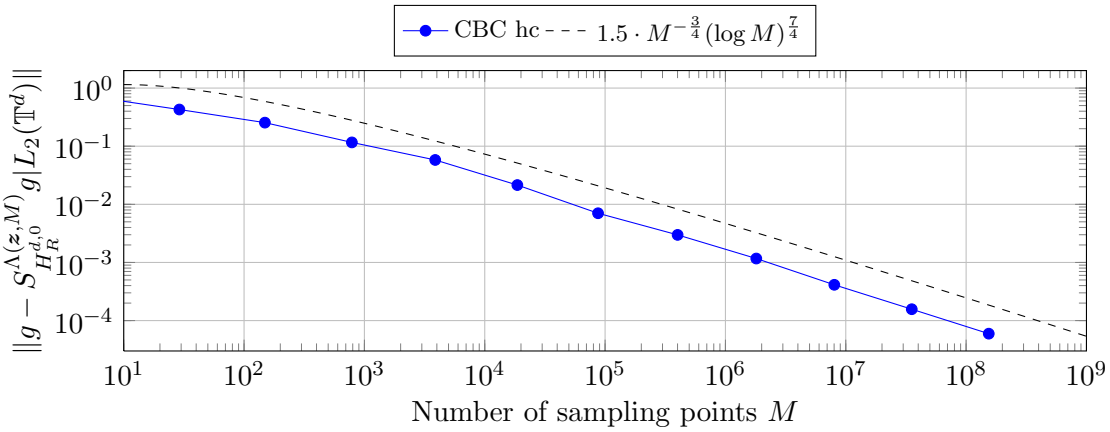

(b) $d = 3$

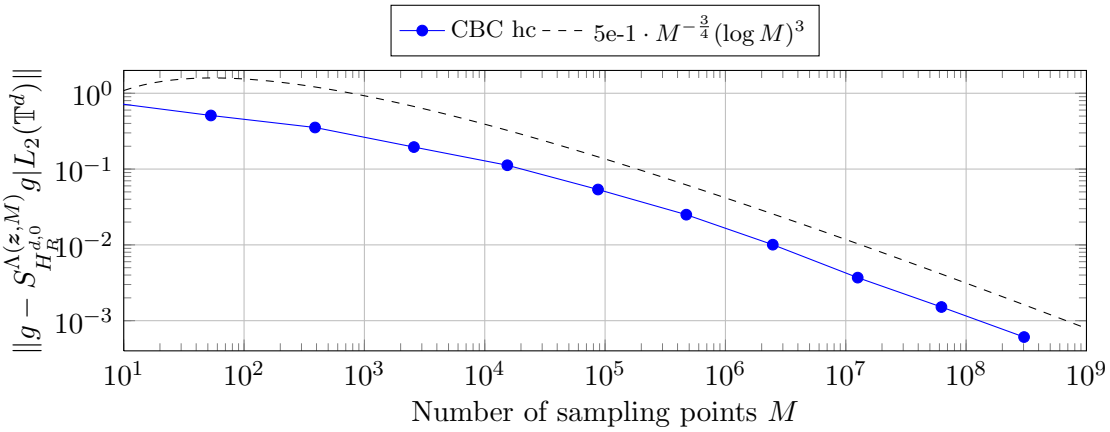

(c) $d = 4$

Figure 8.1: $L_2(\mathbb{T}^d)$ sampling error and number of sampling points for the approximation of the kink function g from (8.1).

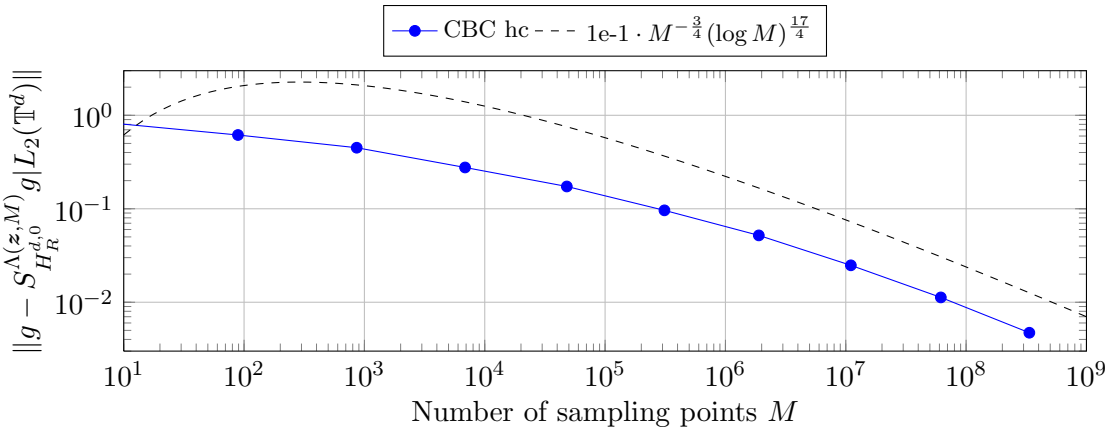

(a) $d = 5$

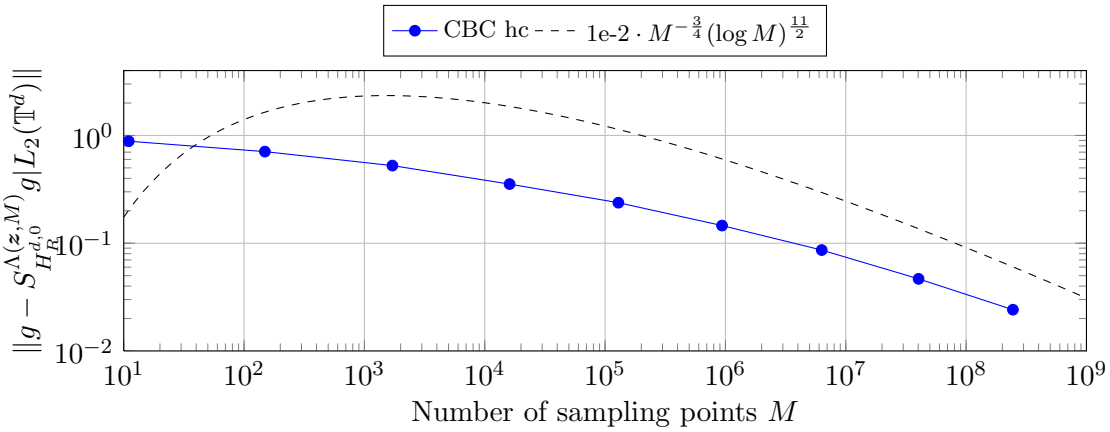

(b) $d = 6$

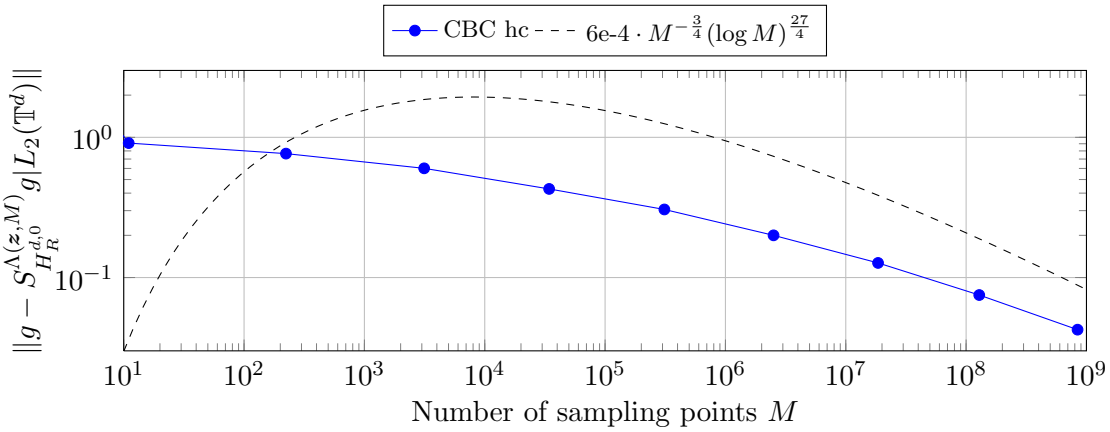

(c) $d = 7$

Figure 8.2: $L_2(\mathbb{T}^d)$ sampling error and number of sampling points for the approximation of the kink function g from (8.1).

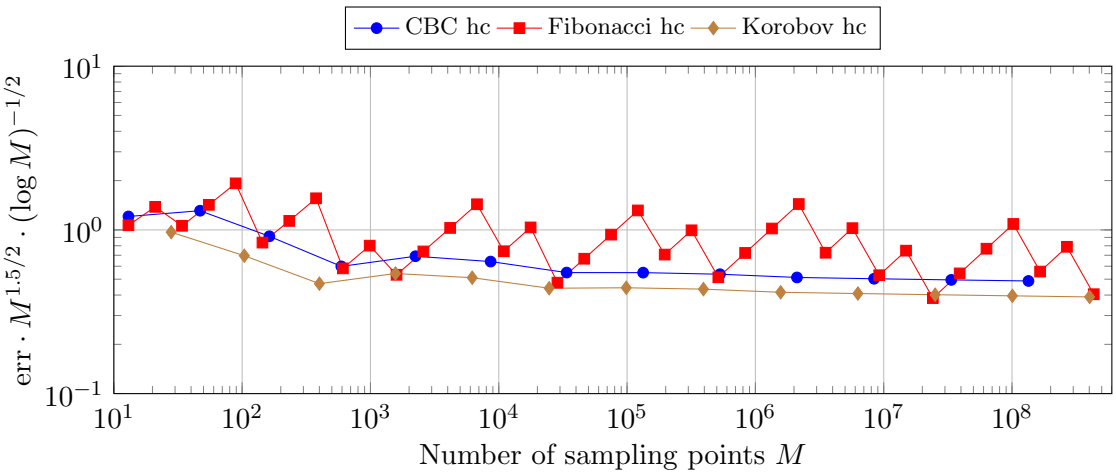

(a) $d = 2$

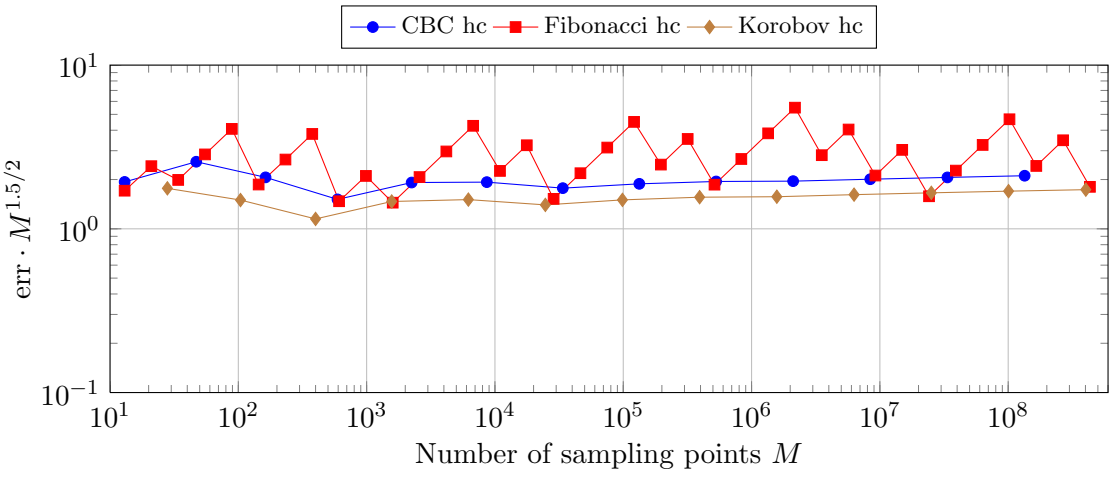

(b) $d = 2$

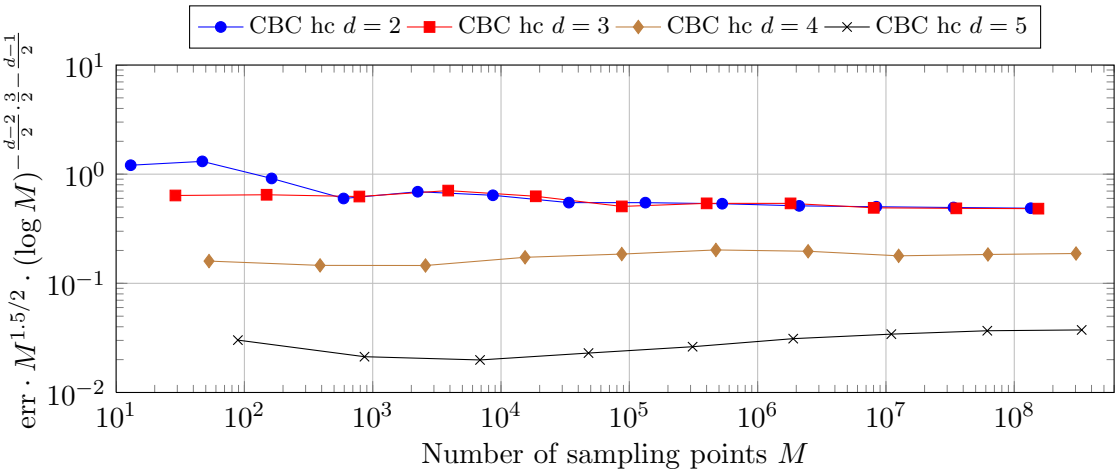
CBC hc $d = 2$
CBC hc $d = 3$
CBC hc $d = 4$
CBC hc $d = 5$
$\mathrm{err} \cdot M^{1.5/2} \cdot (\log M)^{-\frac{d-2}{2} \cdot \frac{3}{2} - \frac{d-1}{2}}$
Number of sampling points M

(c) $d = 2, 3, 4, 5$

Figure 8.3: Scaled $L_2(\mathbb{T}^d)$ sampling error and number of sampling points for the approximation of the kink function g from (8.1), where $\mathrm{err} := \|g - S^{\Lambda(\boldsymbol{z},M)}_{H^{d,0}_R} g | L_2(\mathbb{T}^d)\|$.

8.2 ℓ_∞-ball index sets

Next, we use the lattices from Section 8.1 in the two-dimensional case, but instead of hyperbolic cross index sets $H_R^{2,0}$, we are going to use the ℓ_∞-ball index sets $I_N^2 := \left\{-\left\lceil\frac{N-2}{2}\right\rceil, \ldots, \left\lceil\frac{N-1}{2}\right\rceil\right\}^2$, $N \in \mathbb{N}$. For each of the rank-1 lattices $\Lambda(\boldsymbol{z}, M)$ generated in Section 8.1, we determine the largest refinement $N \in \mathbb{N}$ such that the reconstruction property (2.5) is still fulfilled for the ℓ_∞-ball I_N^2. Then, we apply each sampling operator $S_{I_N^2}^{\Lambda(\boldsymbol{z},M)}$ on the kink function g from (8.1). The resulting sampling errors are depicted in Figure 8.4, where the errors for the CBC, Fibonacci and Korobov rank-1 lattices are denoted by "CBC ℓ_∞-ball", "Fibonacci ℓ_∞-ball" and "Korobov ℓ_∞-ball", respectively. We observe that the $L_2(\mathbb{T}^d)$ sampling errors decay approximately as the rate $M^{-\frac{3}{4}}$ as expected. In more detail, this behaviour may be seen in the scaled error plot in Figure 8.5.

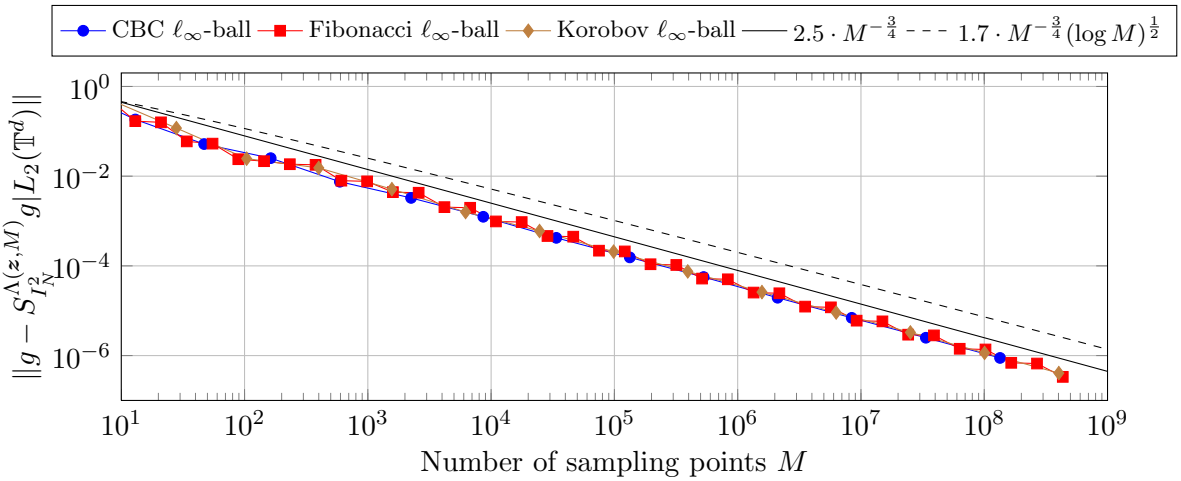

Figure 8.4: $L_2(\mathbb{T}^2)$ sampling error and number of sampling points for the approximation of the kink function g from (8.1).

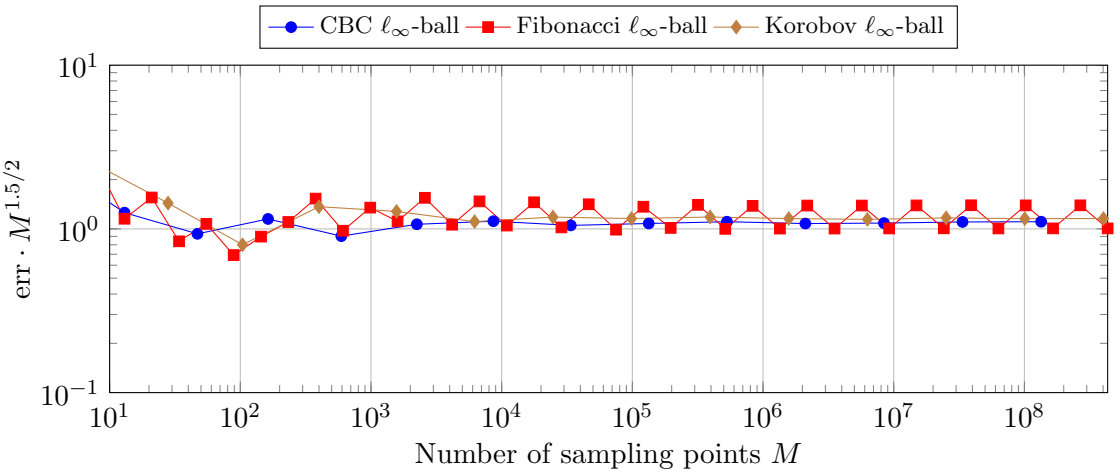

Figure 8.5: Scaled $L_2(\mathbb{T}^2)$ sampling error and number of sampling points for the approximation of the kink function g from (8.1), where err $:= \|g - S_{I_N^2}^{\Lambda(\boldsymbol{z},M)} g | L_2(\mathbb{T}^2)\|$.

Acknowledgements

The authors acknowledge the fruitful discussions with A. Hinrichs, M. Ullrich and R. Bergmann on this topic, especially at the conference "Approximationsmethoden und schnelle Algorithmen" in Hasenwinkel, 2014. Furthermore the authors thank V.N. Temlyakov for his valuable comments and historical hints on that topic. The authors especially thank A. Hinrichs for pointing out an alternative proof argument for the non-optimality of rank-1 lattice sampling, cf. Remark 6.1. Moreover, LK and TV gratefully acknowledge support by the German Research Foundation (DFG) within the Priority Program 1324, project PO 711/10-2. Additionally, GB and TU acknowledge the support by the DFG Emmy-Noether programme (UL403/1-1) and the Hausdorff-Center for Mathematics, University of Bonn.

References

[1] N. S. Bahvalov. Approximate computation of multiple integrals. *Vestnik Moskov. Univ. Ser. Mat. Meh. Astr. Fiz. Him.*, 1959:3–18, 1959.

[2] R. Bergmann. The fast Fourier transform and fast wavelet transform for patterns on the torus. *Appl. Comput. Harmon. Anal.*, 35:39–51, 2013.

[3] H.-J. Bungartz and M. Griebel. Sparse grids. *Acta Numer.*, 13:1–123, 2004.

[4] G. Byrenheid, D. Dũng, W. Sickel, and T. Ullrich. Sampling on energy-norm based sparse grids for the optimal recovery of Sobolev type functions in H^γ. *J. Approx. Theory*, 207:207–231, 2016.

[5] R. Cools, F. Y. Kuo, and D. Nuyens. Constructing lattice rules based on weighted degree of exactness and worst-case error. *Computing*, 87:63–89, 2010.

[6] R. Cools and D. Nuyens. An overview of fast component-by-component constructions of lattice rules and lattice sequences. *PAMM*, 7:1022609–1022610, 2007.

[7] D. Dũng. B-spline quasi-interpolant representations and sampling recovery of functions with mixed smoothness. *J. Complexity*, 27:541–567, 2011.

[8] D. Dũng and T. Ullrich. N-widths and ε-dimensions for high-dimensional approximations. *Found. Comput. Math.*, 13:965–1003, 2013.

[9] D. Dũng. Sampling and Cubature on Sparse Grids Based on a B-spline Quasi-Interpolation. *Found. Comput. Math.*, pages 1–48, 2015.

[10] M. Griebel and J. Hamaekers. Fast discrete Fourier transform on generalized sparse grids. In *Sparse grids and Applications*, volume 97 of *Lecture Notes in Computational Science and Engineering*, pages 75–108. Springer, 2014.

[11] M. Griebel and S. Knapek. Optimized general sparse grid approximation spaces for operator equations. *Math. Comp.*, 78:2223–2257, 2009.

[12] A. Hinrichs, L. Markhasin, J. Oettershagen, and T. Ullrich. Optimal quasi-Monte Carlo rules on higher order digital nets for the numerical integration of multivariate periodic functions. *ArXiv e-prints*, 2015. arXiv:1501.01800 [math.NA].

[13] L. Kämmerer. Reconstructing hyperbolic cross trigonometric polynomials by sampling along rank-1 lattices. *SIAM J. Numer. Anal.*, 51:2773–2796, 2013.

[14] L. Kämmerer. *High dimensional fast Fourier transform based on rank-1 lattice sampling.* Dissertation. Universitätsverlag Chemnitz, 2014.

[15] L. Kämmerer. Reconstructing multivariate trigonometric polynomials from samples along rank-1 lattices. In G. E. Fasshauer and L. L. Schumaker, editors, *Approximation Theory XIV: San Antonio 2013*, pages 255–271. Springer International Publishing, 2014.

[16] L. Kämmerer. Multiple Rank-1 Lattices as Sampling Schemes for Multivariate Trigonometric Polynomials. *Preprint 2015-11, Faculty of Mathematics, Technische Universität Chemnitz*, 2015.

[17] L. Kämmerer, S. Kunis, and D. Potts. Interpolation lattices for hyperbolic cross trigonometric polynomials. *J. Complexity*, 28:76–92, 2012.

[18] L. Kämmerer, D. Potts, and T. Volkmer. Approximation of multivariate periodic functions by trigonometric polynomials based on rank-1 lattice sampling. *J. Complexity*, 31:543–576, 2015.

[19] L. Kämmerer, D. Potts, and T. Volkmer. Approximation of multivariate periodic functions by trigonometric polynomials based on sampling along rank-1 lattice with generating vector of Korobov form. *J. Complexity*, 31:424–456, 2015.

[20] S. Knapek. Approximation und Kompression mit Tensorprodukt-Multiskalenräumen. Dissertation, Universität Bonn, 2000.

[21] N. M. Korobov. Approximate evaluation of repeated integrals. *Dokl. Akad. Nauk SSSR*, 124:1207–1210, 1959.

[22] T. Kühn, S. Mayer, and T. Ullrich. Counting via entropy: new preasymptotics for the approximation numbers of Sobolev embeddings. *ArXiv e-prints*, 2015. arXiv:1505.00631 [math.NA].

[23] T. Kühn, W. Sickel, and T. Ullrich. Approximation numbers of Sobolev embeddings–sharp constants and tractability. *J. Complexity*, 30:95–116, 2014.

[24] T. Kühn, W. Sickel, and T. Ullrich. Approximation of mixed order Sobolev functions on the d-torus — asymptotics, preasymptotics and d-dependence. *Constr. Approx.*, 42:353–398, 2015.

[25] F. Y. Kuo, I. H. Sloan, and H. Woźniakowski. Lattice rules for multivariate approximation in the worst-case setting. In H. Niederreiter and D. Talay, editors, *Monte Carlo and Quasi-Monte Carlo Methods 2004*, pages 289–330. Springer Berlin Heidelberg, Berlin, 2006.

[26] F. Y. Kuo, I. H. Sloan, and H. Woźniakowski. Lattice rule algorithms for multivariate approximation in the average-case setting. *J. Complexity*, 24:283–323, 2008.

[27] F. Y. Kuo, G. W. Wasilkowski, and H. Woźniakowski. Lattice algorithms for multivariate L_∞ approximation in the worst-case setting. *Constr. Approx.*, 30:475–493, 2009.

[28] D. Li and F. J. Hickernell. Trigonometric spectral collocation methods on lattices. In S. Y. Cheng, C.-W. Shu, and T. Tang, editors, *Recent Advances in Scientific Computing and Partial Differential Equations*, volume 330 of *Contemp. Math.*, pages 121–132. AMS, 2003.

[29] H. Niederreiter. Quasi-Monte Carlo methods and pseudo-random numbers. *B. Am. Math. Soc.*, 84:957–1041, 1978.

[30] H.-J. Schmeisser and H. Triebel. *Topics in Fourier analysis and function spaces.* A Wiley-Interscience Publication. John Wiley & Sons, Ltd., Chichester, 1987.

[31] W. Sickel. Approximate recovery of functions and Besov spaces of dominating mixed smoothness. In *Constructive theory of functions*, pages 404–411. DARBA, Sofia, 2003.

[32] W. Sickel. Approximation from sparse grids and function spaces of dominating mixed smoothness. In *Approximation and probability*, volume 72 of *Banach Center Publ.*, pages 271–283. Polish Acad. Sci., Warsaw, 2006.

[33] W. Sickel and T. Ullrich. The Smolyak algorithm, sampling on sparse grids and function spaces of dominating mixed smoothness. *East J. Approx.*, 13:387–425, 2007.

[34] W. Sickel and T. Ullrich. Spline interpolation on sparse grids. *Appl. Anal.*, 90:337–383, 2011.

[35] I. H. Sloan and S. Joe. *Lattice methods for multiple integration.* Oxford Science Publications. The Clarendon Press Oxford University Press, New York, 1994.

[36] I. H. Sloan and A. V. Reztsov. Component-by-component construction of good lattice rules. *Math. Comp.*, 71:263–273, 2002.

[37] V. N. Temlyakov. Reconstruction of periodic functions of several variables from the values at the nodes of number-theoretic nets. *Anal. Math.*, 12:287–305, 1986. In Russian.

[38] V. N. Temlyakov. Approximation of functions with bounded mixed derivative. *Proc. Steklov Inst. Math.*, 1:vi+121, 1989. A translation of Trudy Mat. Inst. Steklov **1**78 (1986), Translated by H. H. McFaden.

[39] V. N. Temlyakov. *Approximation of periodic functions.* Computational Mathematics and Analysis Series. Nova Science Publishers Inc., Commack, NY, 1993.

[40] V. N. Temlyakov. On approximate recovery of functions with bounded mixed derivative. *J. Complexity*, 9:41–59, 1993. Festschrift for Joseph F. Traub, Part I.

[41] T. Ullrich. Smolyak's algorithm, sampling on sparse grids and Sobolev spaces of dominating mixed smoothness. *East J. Approx.*, 14:1–38, 2008.

[42] H. Yserentant. *Regularity and approximability of electronic wave functions*, volume 2000 of *Lecture Notes in Mathematics.* Springer-Verlag, Berlin, 2010.